Research article

Phosphorylation of β-arrestin 2 at Thr^{383} by MEK underlies β-arrestin-dependent activation of Erk1/2 by GPCRs

Elisabeth Cassier[1], Nathalie Gallay[2], Thomas Bourquard[2], Sylvie Claeysen[1], Joël Bockaert[1], Pascale Crépieux[2], Anne Poupon[2], Eric Reiter[2], Philippe Marin[1]*, Franck Vandermoere[1]*

[1] CNRS, UMR-5203, Institut de Génomique Fonctionnelle, F-34094 Montpellier, France; INSERM, U1191, F-34094 Montpellier, France; Université de Montpellier, F-34094 Montpellier, France ; [2] INRA, UMR85, Unité Physiologie de la Reproduction et des Comportements, F-37380 Nouzilly, France ; CNRS, UMR7247, F-37380 Nouzilly, France ; Université François Rabelais, F-37041 Tours, France.

Corresponding authors: Dr Philippe Marin, Institut de Génomique Fonctionnelle, 141 rue de la Cardonille, F-34094 Montpellier Cedex 5, France; Tel +33 434 35 92 13; Fax + 33 467 54 24 32; email: philippe.marin@igf.cnrs.fr; Dr Franck Vandermoere, Institut de Génomique Fonctionnelle, 141 rue de la Cardonille, F-34094 Montpellier Cedex 5, France; Tel +33 434 35 92 13; Fax + 33 467 54 24 32; email: franck.vandermoere@igf.cnrs.fr

Keywords: β-arrestin, Extracellular signal-regulated kinase, G protein-coupled receptor, phosphorylation, mass spectrometry

ABSTRACT

In addition to their role in desensitization and internalization of G protein-coupled receptors (GPCRs), β-arrestins are essential scaffolds linking GPCRs to Erk1/2 signaling. However, their role in GPCR-operated Erk1/2 activation differs between GPCRs and the underlying mechanism remains poorly characterized. Here, we show that activation of serotonin 5-HT_{2C} receptors, which engage Erk1/2 pathway via a β-arrestin-dependent mechanism, promotes MEK-dependent β-arrestin 2 phosphorylation at Thr^{383}, a necessary step for Erk recruitment to the receptor/β-arrestin complex and Erk activation. Likewise, Thr^{383} phosphorylation is involved in β-arrestin-dependent Erk1/2 stimulation elicited by other GPCRs such as β_2-adrenergic, FSH and CXCR4 receptors, but does not affect the β-arrestin-independent Erk1/2 activation by 5-HT_4 receptor. Collectively, these data show that β-arrestin 2 phosphorylation at Thr^{383} underlies β-arrestin-dependent Erk1/2 activation by GPCRs.

INTRODUCTION

Arrestins were initially named on the basis of their ability to turn-off the coupling of G protein-coupled receptors (GPCRs) to G proteins and thereby inhibit G protein-dependent GPCR signaling. Over the last decade, it has become evident that β-arrestins are also important signal transducers and that a number of biological functions exerted by GPCRs are mediated by β-arrestin-dependent signaling *(1-4)*. β-arrestins act as multifunctional scaffolds that recruit multiple signaling molecules, such as the core Extracellular signal-regulated kinase Erk1/2 signaling module, composed of Raf1, MAP kinase kinase MEK1 and MAP kinases Erk1/2, a process leading to Erk1/2 activation *(5-7)*. Typically, most GPCRs induce temporally distinct and spatially segregated G protein-dependent and β-arrestin-dependent activation of Erk: G protein-mediated Erk activation is rapid and transient, reaching a maximal level within a few minutes and is followed by translocation of activated Erk into the nucleus to promote gene transcription and cell proliferation. In contrast, β-arrestin-mediated Erk1/2 activation is slower in onset, requiring 5-10 min to reach maximal level, persists more than one hour and mainly occurs in the cytosol *(5, 8, 9)*. However, Erk1/2 signaling elicited by certain GPCRs does not fit this classic bimodal activation pattern: for example, the activation of Erk1/2 pathway by $5HT_{2C}$ receptors is entirely dependent on β-arrestins *(10)*, whereas the engagement of this pathway by the $5\text{-}HT_4$ receptor does not require β-arrestin recruitment *(11)*. In addition, some GPCRs such as μ-opioid receptor induce β-arrestin-dependent activation of Erk1/2 that translocate to the nucleus *(12)*.

Accumulating evidence indicates that β-arrestin recruitment to GPCRs and engagement of β-arrestin-mediated signaling depend on both receptor conformational state and a complex pattern of receptor phosphorylation elicited by GPCR kinases (GRKs) *(5, 13)*. This phosphorylation barcode is translated into specific β-arrestin conformations that dictate selective signalling and the nature of β-arrestin intracellular functions. Another mechanism that might underlie β-arrestin dependency of receptor-operated signaling is the phosphorylation of β-arrestins themselves. Several phosphorylated residues have been identified in the β-arrestin sequences, including Ser^{412} for β-arrestin 1 *(14-16)* and Thr^{276},

Ser^{361} and Thr^{383} for β-arrestin 2 *(17-19)*. These phosphorylation events affect GPCR internalization and/or sequestration and, consequently, steady-state level of GPCR cell-surface expression: phosphorylation of β-arrestin 1 at Ser^{412} by Erk1/2 as well as the phosphorylation of β-arrestin 2 at both Ser^{361} and Thr^{383} reduce their ability to induce internalization of β_2-adrenergic receptor *(14, 16, 17)*, while phosphorylation of β-arrestin 2 at Ser^{14} and Thr^{276} promotes intracellular sequestration of CXCR4 receptor *(18)*. These results indicate that β-arrestin 2 phosphorylation exerts contrasting effects on GPCR trafficking that may depend on the nature of the phosphorylated residue(s) and of the GPCR. Another phosphorylated site (Ser^{178}) was identified in rat/mouse β-arrestin 2 and its phosphorylation state affects endosomal trafficking of various GPCRs *(20)*. However, this serine residue is not conserved in other species including human, suggesting different regulations of endosomal GPCR trafficking between species. Additional phosphorylated residues have been found on β-arrestin 2 in large-scale phosphoproteomics screens, but their functional relevance remains to be established *(21-26)*. In contrast to its role in GPCR trafficking, the influence of β-arrestin phosphorylation on GPCR-operated β-arrestin-dependent signaling such as Erk1/2 activation remains unexplored.

Here, we investigated the impact on β-arrestin 1 and 2 phosphorylation of expression/stimulation of 5-HT_{2C} and 5-HT_4 receptors, two GPCRs that differ in their β-arrestin dependency to promote Erk1/2 activation, using high-resolution mass spectrometry. We identified several previously described as well as novel phosphorylated residues on β-arrestin 2, while only one phosphorylated site was found on β-arrestin 1. Of these, only phosphorylation of β-arrestin 2 at Thr^{383} exhibited a strong increase upon 5-HT_{2C} receptor stimulation. Furthermore, Thr^{383} was poorly phosphorylated in cells expressing 5-HT_4 receptor and its phosphorylation was only slightly enhanced by agonist treatment. These findings prompted functional studies to evaluate the influence of this phosphorylation event in Erk1/2 phosphorylation elicited by stimulation of 5-HT_{2C} receptor and other GPCRs known to engage Erk signaling in a β-arrestin-dependent manner, in comparison with 5-HT_4 receptor stimulation, which induces Erk1/2 activation through a β-arrestin-independent mechanism.

RESULTS

5-HT_{2C} and 5-HT_4 receptor stimulation induce distinct patterns of β-arrestin phosphorylation

To characterize in a global manner the impact of 5-HT_{2C} and 5-HT_4 receptor expression/stimulation on the phosphorylation state of β-arrestins, YFP-tagged versions of β-arrestin 1 or β-arrestin 2 were co-expressed with Myc-tagged 5-HT_{2C} or 5-HT_4 receptors in HEK-293 cells. Cells were then treated with vehicle or 5-HT for 5 or 30 min. β-arrestins were immunoprecipitated using GFP nanobodies coupled to sepharose beads (GFP-Trap), resolved by SDS-PAGE, detected by colloidal Coomassie blue staining (Figure 1 - Figure supplement 1) and digested in-gel with trypsin. Analysis of the resulting peptides by nano-LC-MS/MS yielded 88% and 85% sequence coverage for β-arrestin 1 and β-arrestin 2, respectively, with a p-value threshold of 0.01 for peptide identification (Figure 1 - Figure supplement 2).

Only one phosphorylated site (Thr^{374}) was identified on β-arrestin 1, but the corresponding phosphorylated peptide was only detected in cells expressing 5-HT_4 receptor, and with a low phosphorylation index, as estimated by dividing the MS signal intensity of the phosphorylated peptide by the sum of MS signal intensities of the phosphorylated and the corresponding non-phosphorylated peptide (Figure 1 - Source data 1, see also the fragmentation spectrum that pinpoints the position of the phosphorylation site on Figure 1 - Figure supplement 3). Moreover, label-free quantification of the MS signal of this phosphorylated peptide in cells treated or not with 5-HT indicated that Thr^{374} phosphorylation is not affected by 5-HT exposure (Figure 1 - Source data 1). Previous studies using a phosphorylated site-specific antibody have identified Ser^{412} as an additional phosphorylated residue on β-arrestin 1 *(14-16)*. They also indicated that Ser^{412} phosphorylation state is modified upon activation of various GPCRs, including the 5-HT_4 receptor *(15)*. Our MS/MS analyses did not identify this phosphorylated residue, but a low-intensity ion signal corresponding to the theoretical m/z of a peptide comprising the phosphorylated Ser^{412} was detected in cells expressing the 5-HT_4 receptor and exposed for 30 min to 5-HT.

Six phosphorylated residues (Thr^{178}, Ser^{194}, $Ser^{267/268}$, Ser^{281}, Ser^{361} and Thr^{383}) were identified on β-arrestin 2 (Figure 1A, Figure 1 - Source data 1 and Figure 1 - Figure supplement 3-5). Note that the fragmentation spectrum of the CPVAQLEQDDQVSPp($S^{267}S^{268}$)TFCK peptide did not provide enough information to discriminate between a phosphorylation at Ser^{267} or at Ser^{268}, but the precursor peptide m/z clearly showed that it carries only one phosphorylated residue (Figure 1 - Figure supplement 3). Relative quantification of MS signals of β-arrestin 2 phosphorylated peptides showed that the phosphorylation of these residues except for Thr^{383} was not affected by 5-HT_{2C} or $5HT_4$ receptor expression or stimulation (Figure 1 - Source data 1). In cells expressing the 5-HT_{2C} receptor, Thr^{383} phosphorylation showed a marked elevation after a 5-min 5-HT stimulation, which persisted 30 min after the onset of the treatment. Thr^{383} phosphorylation slightly but not significantly increased after the 30-min 5-HT challenge in cells expressing 5-HT_4 receptor and was much less pronounced than that measured in presence of 5-HT_{2C} receptor (Figure 1B and Figure 1 - Source data 1). We next examined whether 5-HT_{2C} receptor stimulation likewise induces phosphorylation of endogenous β-arrestin 2 at Thr^{383}, but did not detect any ion signal corresponding to the phosphorylated peptide comprising this residue in cells not transfected with the YFP-β-arrestin 2 plasmid. We thus generated a polyclonal antibody that specifically recognizes β-arrestin 2 phosphorylated at Thr^{383} (see Figure 2C and Figure 2 - Source data 1). Western blot experiments using this antibody showed that 5-HT_{2C} receptor stimulation induces a substantial increase in endogenous β-arrestin 2 phosphorylation at Thr^{383}, while activation of the 5-HT_4 receptor did not affect its phosphorylation level (Figure 1C and Figure 1 - Source data 2), corroborating the MS/MS analysis of ectopic β-arrestin 2 phosphorylation.

Role of MEK in β-arrestin 2 phosphorylation at Thr^{383} elicited by 5-HT_{2C} receptor stimulation

Given the strong enhancement of Thr^{383} phosphorylation induced by the stimulation of 5-HT_{2C} receptor that parallels the β-arrestin 2-dependent receptor-operated activation of Erk1/2 (Figure 1 and Figure 1 - Figure supplement 1), we paid particular attention to the

phosphorylation of this residue, which is located in an unfolded region of the carboxy-terminal region of β-arrestin 2 easily accessible to protein kinases (Figure 1A). In an effort to identify kinase(s) involved in its phosphorylation, we first used Group-based Prediction System (GPS, v2.1), an algorithm for kinase consensus search that classifies protein kinases into a hierarchical structure with four levels and trains against the PhosphoELM database, in order to determine individual false discovery rates for each of them *(27)*. GPS search revealed that Thr^{383} is a strong consensus for phosphorylation by casein kinase 2 (CK2 GPS score 5.3), consistent with previous findings *(17, 19)*. However, neither basal nor 5-HT_{2C} receptor-elicited Thr^{383} phosphorylation was affected by treating cells with the selective cell-permeable CK2 pharmacological inhibitor tetrabromocinnamic acid (TBCA, Figure 2 - Figure supplement 1 and Figure 2 - Figure supplement 1 – Source data 1) *(28)*, indicating a marginal contribution of CK2 in the phosphorylation of this residue in living HEK-293 cells. GPS search also suggested that Thr^{383} is a potential site for phosphorylation by MAP2K1 (MEK1, GPS score 6.0). Numerous studies have shown that β-arrestins associated with a GPCR can interact with different signaling proteins including c-Src and several proteins of the Erk signaling module (Raf/MEK/Erk), and that these interactions depend on β-arrestin conformational state *(29, 30)*.

In line with these findings, we have recently modeled the complex between a GPCR, β-arrestin 2, c-Src and the Erk module from the 3D structure of each partner, using the Protein-Protein cOmplexes 3D structure pRediction (PRIOR) docking algorithm, and validated experimentally the previously unknown interaction regions *(31)*. This model predicts that the unfolded C-terminal part of β-arrestin comprising Thr^{383} is located in the vicinity of the MEK active site (Figure 2A), indicating a possible role of MEK bound to β-arrestin 2 in its phosphorylation. Based on this model, we hypothesized that the mechanism of β-arrestin-dependent activation of Erk consists in the following steps: (i) Raf and MEK assemble to β-arrestin 2 bound to agonist-stimulated receptor, resulting in MEK activation, (ii) MEK phosphorylates β-arrestin 2 at Thr^{383}, resulting in a large conformational change of the β-arrestin 2 region comprising residues 350-393, (iii) the receptor C-terminus associates with β-

arrestin 2 using the region previously occupied by the 383-393 β-strand within the β-arrestin 2 C-terminal tail and (iv) Erk binds to the complex and can be activated by MEK (Figure 2A). Consistent with this hypothesis, pretreatment of cells with the MEK pharmacological inhibitor U0126 (5 μM) abolished Thr^{383} phosphorylation elicited by 5-HT_{2C} receptor stimulation (Figure 2B and Figure 2 - Source data 1). Expression of a MEK1 dominant-negative inhibitor (MEK1DN) also strongly reduced Thr^{383} phosphorylation state (Figure 2B, see also Figure 2 - Figure supplement 2 for controls showing strong MEK inhibition induced by both approaches, as assessed by monitoring phosphorylation of Erk1/2). In contrast, pretreating cells with FR180204 (10 μM), a selective pharmacological inhibitor of Erk1/2, did not affect Thr^{383} phosphorylation (Figure 2B). The ability of FR180204 treatment to inhibit Erk1/2 activity without affecting MEK activity in our experimental conditions was assessed by monitoring phosphorylation of Erk1/2 and their substrate Elk1 (Figure 2 - Figure supplement 2). Collectively, these results identify MEK as the major kinase involved in phosphorylation of β-arrestin 2 at Thr^{383} upon 5-HT_{2C} receptor stimulation. To further confirm the ability of MEK to directly phosphorylate this residue, we performed an *in vitro* kinase assay using purified active MEK1 and YFP-β-arrestin 2 purified from transfected HEK-293 cells as substrate, followed by Western blotting using the anti-phospho-Thr^{383} β-arrestin 2 antibody. MEK1 induced a strong elevation in the immunoreactive signal that was abolished by adding U0126 in the incubation medium (Figure 2C). As expected, no increase in immunoreactive signal was observed in experiments using YFP-Thr^{383}Ala β-arrestin 2 mutant as substrate, thus validating the specificity of the antibody for β-arrestin2 phosphorylated at Thr^{383}. This result was confirmed using a radioactive kinase assay, which also showed comparable efficacy of MEK1 to promote phosphorylation of purified β-arrestin 2 and its canonical substrate Erk2 *in vitro* (Figure 2 - Figure supplement 3 and Figure 2 - Figure supplement 3 – Source data 1).

β-arrestin 2 phosphorylation at Thr^{383} neither affects translocation of β-arrestin 2 to 5-HT_{2C} and 5-HT_4 receptors nor agonist-induced receptor internalization

To explore whether Thr^{383} phosphorylation affects the recruitment of β-arrestin 2 by 5-HT_{2C} and 5-HT_4 receptors, we monitored interaction between each receptor and either wild type or Thr^{383}Ala or Thr^{383}Asp β-arrestin 2 mutants using a BRET-based assay. Exposure of cells to 5-HT induced a strong increase in the BRET signal between 5-HT_{2C}-YFP or 5-HT_4-YFP receptor and Rluc-β-arrestin 2 (Figures 3A, 3B and Figure 3 - Source data 1). The 5-HT-elicited BRET signal was similar in cells expressing wild type β-arrestin 2, Thr^{383}Ala or Thr^{383}Asp β-arrestin 2 mutants, indicating that Thr^{383} phosphorylation does not affect β-arrestin 2 translocation to either receptor. Likewise, 5-HT treatment decreased cell surface expression of 5-HT_{2C} and 5-HT_4 receptors to a similar extent in cells expressing wild type β-arrestin 2, Thr^{383}Ala or Thr^{383}Asp β-arrestin 2 mutants (Figures 3C and D), indicating that Thr^{383} phosphorylation does not affect agonist-induced internalization of these receptors.

Impact of Thr^{383} phosphorylation upon β-arrestin 2 conformational changes elicited by 5-HT_{2C} and 5-HT_4 receptor stimulation

β-arrestins are known to undergo important conformational rearrangements upon translocation to agonist-stimulated GPCRs that are essential for their downstream action *(29, 32)*. To explore the impact of Thr^{383} phosphorylation on conformational changes of β-arrestin 2 induced by 5-HT_{2C} receptor activation *vs.* 5-HT_4 receptor activation, we used an optimized intramolecular BRET biosensor consisting of β-arrestin 2 sandwiched between the *Renilla* green fluorescent protein (RGFP) and the *Renilla* luciferase variant Rluc8 *(33, 34)*. When β-arrestin 2 conformation changes, the distance between Rluc8 and RGFP increases or decreases leading to a BRET signal decrease or increase. Treating cells coexpressing 5-HT_{2C} receptor and WT RLuc8-β-arrestin 2-RGFP with 5-HT increased the BRET signal. No BRET increase was detected upon agonist exposure in cells coexpressing the receptor and T^{383}A RLuc8-β-arrestin 2-RGFP (Figure 3E). Mutation of Thr^{383} into aspartate in RLuc8-β-arrestin 2-RGFP also resulted in an increase in BRET signal to a level similar to the one measured in cells expressing the wild type probe and exposed to 5-HT, and 5-HT treatment did not further enhance this elevated BRET signal (Figure 3E). In contrast, substitution of Thr^{383} by alanine or aspartate did not affect the increase in RLuc8-β-arrestin 2-RGFP BRET signal induced by

5-HT treatment in cells expressing 5-HT_4 receptors (Figure 3F). Collectively, these results indicate that β-arrestin 2 conformational change elicited by 5-HT_{2C} receptor stimulation, but not 5-HT_4 receptor stimulation, depends on Thr^{383} phosphorylation.

β-arrestin 2 phosphorylation at Thr^{383} is essential for Erk1/2 translocation to the 5-HT_{2C} receptor/β-arrestin 2 complex

As previously hypothesized, it can be envisioned that the unfolded C-terminal region of β-arrestin 2 occupies the docking site of Erk1/2 located in the vicinity of MEK catalytic site in the receptor/β-arrestin 2 complex (Figure 2A). Consequently, Thr^{383} phosphorylation status might affect Erk1/2 recruitment. In fact, our model predicts that Thr^{383} phosphorylation should induce a movement of the β-arrestin 2 C-terminal region away from the complex leaving space for further recruitment of Erk (Figure 2A). To explore this possibility, we compared the ability of wild type and Thr^{383}Ala and Thr^{383}Asp β-arrestin 2 to recruit Erk1/2 upon 5-HT_{2C} receptor stimulation by co-immunoprecipitation. Treating 5-HT_{2C} receptor-expressing cells with 5-HT increased the amount of Erk1/2 co-immunoprecipitated with β-arrestin 2, an effect abolished by mutating Thr^{383} into Ala (Figure 4A and Figure 4 - Source data 1). In contrast, mutation of Thr^{383} into aspartate increased Erk1/2 recruitment by β-arrestin 2 even in the absence of the agonist and receptor stimulation did not induce any additional effect (Figure 4A). Further supporting a role of Thr^{383} phosphorylation by MEK, treatment of cells with U0126 prevented recruitment of Erk1,2 by β-arrestin 2 induced by 5-HT_{2C} receptor stimulation (Figure 4 - Figure supplement 1 and Figure 4 - Figure supplement 1 - Source data 1). 5-HT did not promote Erk1/2 recruitment by β-arrestin 2 in cells coexpressing 5-HT_4 receptor and either wild type or mutated forms of β-arrestin 2 (Figure 4B). Collectively, these results suggest that Thr^{383} phosphorylation by MEK promotes a conformational change of β-arrestin 2 that facilitates Erk recruitment by the 5-HT_{2C} receptor/β-arrestin 2 complex, whereas it has no influence upon its translocation to the 5-HT_4 receptor/β-arrestin 2 complex.

Role of Thr^{383} phosphorylation in 5-HT$_{2C}$ receptor-operated Erk1/2 signaling

In line with the role of Thr^{383} phosphorylation in Erk recruitment by the 5-HT$_{2C}$ receptor/β-arrestin 2 complex, we next explored the influence of this phosphorylation event in receptor-operated Erk1/2 activation, which has previously been reported to depend on β-arrestin 2 *(10)*. The ability of 5-HT (both 5- and 30-min exposures) to promote Erk1/2 phosphorylation was strongly reduced in cells co-expressing 5-HT$_{2C}$ receptor and T^{383}A β-arrestin 2, compared with cells expressing WT β-arrestin 2 (Figure 4C). Likewise, Erk1/2 phosphorylation was reduced in non-stimulated cells expressing T^{383}A β-arrestin 2, while expression of T^{383}D β-arrestin 2 increased basal Erk1/2 phosphorylation to a level that was not further increased by agonist treatment. Altogether, these results identify Thr^{383} phosphorylation as a key event contributing to basal and 5-HT$_{2C}$ receptor-operated Erk1/2 activation. In contrast and consistent with the β-arrestin-independent 5-HT$_4$ receptor-operated Erk signaling *(11)*, mutating Thr^{383} into alanine or aspartate did not affect Erk1/2 phosphorylation elicited by 5-HT$_4$ receptor stimulation (Figure 4D).

Role of Thr^{383} phosphorylation in Erk1/2 signaling elicited by other GPCRs

We next explored the impact of Thr^{383} phosphorylation on Erk1/2 activation induced by stimulation of other GPCRs known to engage the Erk pathway via the classic dual mechanism involving both G protein- and β-arrestin-dependent pathways, namely follicle-stimulating hormone (FSH) receptor, β-adrenergic receptors and chemokine CXCR4 receptor *(9, 35, 36)*. Consistent with our previous findings *(35)*, silencing β-arrestin 2 expression strongly reduced the level of Erk1/2 phosphorylation elicited by exposing cells transiently expressing FSH receptor to FSH for 30 min, whereas it only slightly but not significantly affected Erk1/2 phosphorylation induced by a 5-min FSH treatment (Figure 5A, see also Figure 5 - Figure supplement 1, Figure 5 – Source data 1 and Figure 5 - Figure supplement 1 - Source data 1). Erk1/2 phosphorylation level measured after a 30-min FSH treatment was also significantly diminished in cells expressing T^{383}A β-arrestin 2, compared with WT β-arrestin 2 (Figure 5D). Likewise, Erk1/2 phosphorylation elicited by stimulating endogenously expressed β-adrenergic receptor by isoproterenol or CXCR4 receptor by CXCL12 was reduced to a similar

extend by silencing β-arrestin 2 expression (Figures 5B,C) or by substituting Thr^{383} by alanine (Figures 5E,F). Collectively, these results indicate that Thr^{383} substitution by alanine reproduces the inhibitory effect of β-arrestin 2 down-regulation upon activation of Erk1/2 by the three GPCRs examined, suggesting that phosphorylation of this residue is a general mechanism underlying β-arrestin-dependent Erk1/2 activation by GPCRs.

DISCUSSION

In this study, using high-resolution mass spectrometry combined with label-free quantification, we provide for the first time a comprehensive characterization of phosphorylated sites on β-arrestins 1 and 2 in living cells. We also explored the influence on their phosphorylation status of 5-HT_{2C} and 5-HT_4 receptors, two model GPCRs that engage the Erk1/2 pathway through β-arrestin-dependent and independent mechanisms, respectively. We identified one phosphorylated site on β-arrestin 1 and six on β-arrestin 2, including three previously identified residues (Ser^{178}, Ser^{361} and Thr^{383}) and three new sites (Ser^{194}, $Ser^{267/268}$ and Ser^{281}). Two of the β-arrestin 2 phosphorylated sites identified (Ser^{194}, $Ser^{267/268}$) are conserved in β-arrestin 1, but we did not detect the corresponding phosphorylated peptides in β-arrestin 1. Though MS/MS does not allow exhaustive identification of peptides present in complex samples, it is unlikely that our analyses, which covered about of 85 % of the sequence of both arrestins, missed these phosphorylated residues on β-arrestin 1 or any other robustly phosphorylated residues on both arrestins. Therefore, our results corroborate previous findings which identified much more phosphorylated residues on β-arrestin 2 than on β-arrestin 1 and suggest that β-arrestin 2 is phosphorylated at higher stoichiometry, compared with β-arrestin 1. Our analyses did not detect, even in 5-HT-treated cells, another site conserved between both β-arrestins (Ser^{276}) that was previously reported as being phosphorylated by recombinant active Erk1 in an *in vitro* phosphorylation assay followed by MS/MS analysis *(18)*. This suggests that in cells expressing 5-HT_{2C} or 5-HT_4 receptor, the level of Erk1/2 activity and/or the molecular environment of this serine residue do not allow its phosphorylation at high stoichiometry.

Amongst β-arrestin 2 phosphorylated residues identified in the present study, only the phosphorylation of Thr^{383} was modulated upon agonist stimulation of 5-HT_{2C} receptor and, to a much lesser extent, 5-HT_4 receptor. *In silico* search of kinase-specific phosphorylation sites in β-arrestin 2 sequence identified Thr^{383} as a strong consensus for phosphorylation by CK2, consistent with previous findings which showed that Thr^{383} is phosphorylated by CK2 *in vitro (19)*, and by MEK. Our results indicate that MEK rather than CK2 is involved in Thr^{383} phosphorylation elicited by 5-HT_{2C} receptor stimulation in living HEK-293 cells, consistent with our docking model of the receptor/β-arrestin 2/MEK complex, which predicts that the unfolded C-terminal part of β-arrestin comprising Thr^{383} is located in the vicinity of MEK active site.

In an effort to characterize the functional impact of Thr^{383} phosphorylation, we found that its replacement by alanine or aspartate to inhibit or mimic its phosphorylation, did not modify β-arrestin 2 translocation to the receptor nor agonist-induced receptor internalization. This result corroborates previous observations indicating that the sole substitution of Thr^{383} to aspartate or alanine does not affect isoproterenol-induced β_2-adrenergic receptor internalization *(17)*. In fact, only the double substitution of Ser^{361} and Thr^{383} to aspartate inhibited agonist-induced receptor internalization, an effect reflecting the reduced ability of this double β-arrestin mutant to bind to clathrin *(17)*. It is likely that the phosphorylation stoichiometry of Ser^{361} and Thr^{383} in our experimental conditions, including cells exposed to 5-HT, does not allow such a regulation. Moreover, previous studies showed that β_2-adrenergic receptor stimulation decreases rather than enhances the phosphorylation of these residues *(17, 19)*. Accordingly, these studies and our results suggest that β-arrestin 2 phosphorylation at Thr^{383} might only have a minor influence on GPCR trafficking. In contrast, expressing Thr^{276}Ala or Ser^{14}Ala β-arrestin 2 mutants in β-arrestin 1/2 knockout cells fails to restore agonist-induced CXCR4 receptor sequestration while expressing a β-arrestin 2 mutant harboring an aspartate at these positions is sufficient to decrease cell surface localization in the absence of agonist *(18)*. This suggests that Thr^{276} and/or Ser^{14} phosphorylation rather than Thr^{383} phosphorylation might be critical for agonist-induced intracellular sequestration of some GPCRs.

Our results establish a causal link between Thr^{383} phosphorylation and β-arrestin 2 conformational rearrangements, assessed by double brilliance BRET assay, elicited upon 5-HT_{2C} receptor stimulation. They corroborate previous observations suggesting that conformational changes of β-arrestin do not directly result from its binding to phosphorylated GPCRs, but from downstream events, such as subsequent recruitment of β-arrestin interacting proteins *(34, 37)*. Nonetheless, Thr^{383} phosphorylation dependency of β-arrestin 2 conformational changes seems to also depend on the nature of the GPCR it associates with, as the increase in intramolecular BRET signal measured upon 5-HT_4 receptor stimulation was not affected by substituting Thr^{383} by alanine or by aspartate.

The present study also identified Thr^{383} phosphorylation as an essential molecular step allowing Erk1/2 translocation to the 5-HT_{2C}/β-arrestin2/MEK complex and subsequent activation of Erk1/2 signaling upon 5-HT_{2C} receptor stimulation. Based on the current experimental results and our previously validated docking model *(31)*, we propose a molecular mechanism which might explain the role of Thr^{383} phosphorylation in recruitment and activation of Erk at the activated β-arrestin. In the crystal structures of both β-arrestin 1 (PDB 1G4R) *(38)* and β-arrestin 2 (PDB 3P2D) *(39)*, the segment of the C-terminal tail comprising residues 385-393 folds as a β-strand, which associates with the first N-terminal β-strand. The crystal structure of β-arrestin 1 in complex with a C-terminal peptide of the V2 receptor (PDB 4JQI) *(40)*, also shows that the C-terminal peptide of the receptor occupies the same location as the 385-393 segment of the inactive β-arrestin. Consequently, a drastic conformational change of the 385-393 β-arrestin segment is necessary for the correct association of β-arrestin with the receptor. Furthermore, our previously reported docking model shows that the C-terminal region of the receptor is sandwiched between β-arrestin and Erk, and thus has to associate with β-arrestin before its association with Erk *(31)*. Finally, although Thr^{383} is not present in the different structures of β-arrestins, the position of Asp^{385} shows that Thr^{383} is located in the vicinity of β-arrestin-bound MEK's active site, where it can be phosphorylated. In our model (Figures 2 and 6), Thr^{383} phosphorylation by MEK takes place within the ligand-dependent receptor/β-arrestin/Raf/MEK complex. We propose that

this phosphorylation triggers the conformational change of the 350-393 region, allowing the interaction of β-arrestin with the receptor C-terminal domain, the subsequent binding of Erk to the complex and its activation by MEK.

This mechanism, initially established for the 5-HT_{2C} receptor, a GPCR which elicits Erk1/2 signaling mainly through a β-arrestin-dependent mechanism, appears to be conserved among GPCRs that induce Erk1/2 activation through the classic dual mechanism involving both G proteins and β-arrestins, such as β-adrenergic, CXCR4 and FSH receptors. Actually, the sustained Erk1/2 phosphorylation induced by agonist stimulation of these receptors was strongly reduced in cells expressing the Thr^{383}Ala β-arrestin 2 mutant. In contrast, substitution of Thr^{383} by aspartate increased the basal level of Erk1/2 phosphorylation, suggesting that phosphorylated β-arrestin 2 can recruit and subsequently activate Erk1/2 in absence of receptor stimulation. As expected, 5-HT_4 receptor-operated Erk1/2 phosphorylation, which is β-arrestin-independent, was not affected by substituting Thr^{383} by alanine. This result is consistent with the low Thr^{383} phosphorylation level measured in cells expressing 5-HT_4 receptors, compared with cells expressing 5-HT_{2C}, and suggests that Thr^{383} phosphorylation might be a key molecular event governing β-arrestin dependency of Erk1/2 pathway engagement by GPCRs.

In conclusion, our study identifies MEK-elicited β-arrestin 2 phosphorylation at Thr^{383} as a key molecular event underlying β-arrestin-dependent Erk1/2 activation by GPCRs. Thr^{383} phosphorylation has recently been involved in β-arrestin 2 association with transient receptor potential vanilloid 1 (TRPV1) at the plasma membrane, which is critical for its role in regulating receptor desensitization *(41)*. This underscores the potentially high influence of Thr^{383} phosphorylation upon various β-arrestin 2 functions related or not to GPCRs, while the phosphorylation of other residues (Ser^{14} and Thr^{276}) might govern steady state level of GPCR cell-surface expression *(18)*. This also indicates that β-arrestin 2 can integrate upstream signals not only *via* its conformational changes upon association with receptors but also through a complex phosphorylation pattern that dictates downstream signaling events and the associated physiological functions.

MATERIALS AND METHODS

Materials

Human Embryonic Kidney-293 (HEK-293) N type cells (RRID:CVCL_0045) were from the American Type Culture Collection (ATCC, CRL-1573^{TM}). All experiments of the study were performed using a previously characterized batch of cells (Isolate #3) *(42)*. Their negative mycoplasma status was analyzed every month using the MycoAlert™ Mycoplasma Detection Kit (Lonza). Culture media were from Invitrogen. The siRNA used to target β-arrestin 2 (5'-AAGGACCGCAAAGUGUUUGUG-3', position 201-221) and the control siRNA (5'-AAUUCUCCGAACGUGUCACGU-3') were from Dharmacon and the GeneSilencer siRNA transfection reagent from Genlantis.

pEYFP-βARR2, pEYFP-βARR1 and pcDNA3-Rluc-βARR2 plasmids were kindly provided by Dr. Michel Bouvier (University of Montreal). pcDNA3-Rluc-βARR2^{T383A} and pcDNA3-Rluc-βARR2^{T383D} constructs were generated by site directed mutagenesis from the pcDNA3-Rluc-βARR2 vector. The pCMV-Rluc8-βARR2-RGFP construct used to monitor β-arrestin 2 conformational changes (double brilliance assays), previously described in *(33)*, was a generous gift from Dr. Ralph Jockers (Institut Cochin, Paris). pCMV-Rluc8-βARR2^{T383A}-RGFP and pCMV-Rluc8-βARR2^{T383D}-RGFP were generated by site directed mutagenesis from this vector. Plasmids encoding Myc-5-HT$_{2C}$-YFP receptor (pEYFP-N1-Myc-5-HT$_{2C}$) and Myc-5-HT$_4$-YFP receptor (pEYFP-N1-Myc-5-HT$_4$) were generated from pRK5-Myc-5-HT$_{2C\text{-}VGV}$ and pRK5-Myc-5-HT$_4$ plasmids *(43, 44)*, respectively. The pcDNA3.1-Flag-FSHR plasmid was described in *(45)*. The plasmid encoding catalytically inactive dominant inhibitory mutant of MEK1 (K97A) was a generous gift from Dr. Robert J. Lefkowitz (Duke University Medical Center, Durham, NC).

The mouse anti-phospho-Thr^{202}/Tyr^{204}-Erk1/2 antibody (Clone E.4, AB_2636855), the rabbit anti-GAPDH antibody (RRID:AB_10167668) and the goat anti-integrin β1 antibody (RRID:AB_2128200) were from Santa Cruz, the rabbit anti-pan arrestin antibody

(RRID:AB_303409) and the mouse anti-β-arrestin 2 antibody (RRID:AB_2060273) from Abcam, the rabbit anti-Erk1/2 antibody (RRID:AB_330744), the rabbit anti-Elk1 (RRID:AB_2277936) and the rabbit anti-phospho-Ser^{383}-Elk1 (RRID:AB_2099016) from Cell Signaling Technology, the rabbit anti-GFP antibody (RRID:AB_221569) from Invitrogen, and the rabbit anti-Flag (RRID:AB_439687) and mouse anti-Myc (RRID:AB_439694) antibodies from Sigma Aldrich. The anti-phosphoThr^{383}- β-arrestin 2 antibody was generated by immunizing rabbits with the synthetic CDTNYAT(PO_3H_2)DDDIVF peptide coupled to Keyhole Limpet Hemocyanin (KLH, Cisbio Bioassays). Antibodies were purified by two consecutive affinity chromatographies. A first chromatography against the immobilized phosphorylated CDTNYAT(PO_3H_2)DDDIVF peptide as bait bound antibodies recognizing both phosphorylated and non-phosphorylated forms of the peptide. The retained fraction was then eluted and used for a second chromatography against the immobilized non-phosphorylated CDTNYATDDDIVF peptide as bait. We considered that the non-retained fraction contains antibodies recognizing β-arrestin 2 phosphorylated at Thr^{383}. 5-HT, isoproterenol and human recombinant FSH were from Sigma Aldrich, U0126 from Promega, FR180204 and TBCA from Tocris and CXCL12 from R&D Systems. [γ-^{32}P]-ATP was from Perkin Elmer.

Cell cultures and transfections

HEK-293 cells, grown in Dulbecco's modified Eagle's medium (DMEM) supplemented with 10% dialyzed, heat-inactivated fetal calf serum and antibiotics, were transfected at 40-50% confluence using polyethyleneimine (PEI, Sigma Aldrich), as previously described *(46)* and used 48 h after transfection. Non-saturating [^{3}H]-mesulergine and [^{3}H]-GR113808 binding experiments showed that 5-HT_{2C} and 5-HT_4 receptor densities in transfected HEK-293 cells were 0.29 and 0.90 pmol/mg protein, respectively. Based on previously published levels of the endogenous β-arrestins in HEK-293 cells *(47)*, we also estimated levels of β-arrestin 1 and β-arrestin 2 as ~1,600 pmol/mg protein and ~300 pmol/mg protein in cells transfected with pEYFP-βARR1 and pEYFP-βARR2 plasmids, respectively, by Western blotting using the rabbit anti-pan arrestin antibody. For experiments using siRNAs, cells were simultaneously

transfected with control or β-arrestin 2 siRNA (150 nmol/10^6 cells) and plasmids encoding receptors of interest, using the GeneSilencer reagent.

Quantitative mass spectrometry analysis of β-arrestin 1 and β-arrestin 2 phosphorylation

HEK-293 cells transiently co-expressing YFP-tagged β-arrestin 1 or YFP-tagged β-arrestin 2 and either Myc-5-HT_{2C} or Myc-5-HT_4 receptor were starved of serum for 4 h, challenged with either vehicle or 5-HT and lysed in 10 mM Tris-HCl, pH 7.4, 150 mM NaCl, 0.5 mM EDTA, 0.5% NP40, 0.4% dodecylmaltoside, 10 mM sodium fluoride, 1 mM sodium pyrophosphate, 50 mM β-glycerophosphate, 2 mM sodium orthovanadate and a protease inhibitor cocktail (Roche). Samples were centrifuged at 15,000 × g for 15 min at 4°C and β-arrestins were immunoprecipitated with agarose-conjugated GFP trap (ChromoTek). After reduction with dithiothreitol (10 mM, 30 min at 60°C) and alkylation with iodoacetamide (50 mM, 45 min at 25°C), immunoprecipitated β-arrestins were resolved by SDS-PAGE and digested in-gel overnight at 25°C with trypsin (1 µg, Gold, Promega). Peptides were analyzed by nano-LC-FT-MS/MS using a LTQ Orbitrap Velos mass spectrometer coupled to an Ultimate 3000 HPLC (Thermo Fisher Scientific). Desalting and pre-concentration of samples were performed on-line on a Pepmap® precolumn (0.3 mm × 10 mm, Dionex). A gradient consisting of 2-40% buffer B (3-33 min), 40-80% B (33–34 min), 80-0% B (49-50 min), and equilibrated for 20 min in 0% B (50-70 min) was used to elute peptides at 300 nL/min from a Pepmap® capillary (0.075 mm × 150 mm) reversed-phase column (LC Packings). Mass spectra were acquired using a top-10 collision-induced dissociation (CID) data-dependent acquisition (DDA) method. The LTQ-Orbitrap was programmed to perform a Fourier transform (FT) full scan (60,000 resolution) on 400-1,400 Th mass range with the top ten ions from each scan selected for LTQ-MS/MS with multistage activation on the neutral loss of 24.49, 32.66 and 48.99 Th. FT spectra were internally calibrated using a single lock mass (445.1200 Th). Target ion numbers were 500,000 for FT full scan on the Orbitrap and 10, 000 MSn on the LTQ. Precursor mass and top 6 per 30 Da windows peak lists were extracted from MS2 using MSconvert 3.0 and searched with Mascot 2.4 (RRID:SCR_014322) against

the same human Complete Proteome Set database (RRID:SCR_002380), cysteine carbamidomethylation as a fixed modification and phosphorylation of Ser, Thr and Tyr as variable modifications, 7 ppm precursor mass tolerance, 0.5 Da fragment mass tolerance and trypsin/P digestion. MS2 spectra matching phosphorylated peptides with ion score over 15 were manually inspected for unique transitions that pinpoint the position of phosphorylation sites. Ion signals corresponding to phosphorylated peptides were quantified from the maximal intensities measured in their ion chromatograms manually extracted using Qual browser v2.1 (Thermo Fisher Scientific) with a tolerance of 5 ppm for mass deviation, and normalized to signals of their non-phosphorylated counterparts. For each identified phosphorylated residue, a phosphorylation index (maximal intensity observed in the phosphorylated peptide extracted ion chromatogram / sum of the maximal intensities observed in the phosphorylated and the non-phosphorylated peptide extracted ion chromatograms) was calculated.

In vitro kinase assays

YFP-tagged β-arrestin 2 (wild type or $Thr^{383}Ala$ mutant) was purified from HEK-293 cells using GFP trap beads, as described in the previous section. For kinase assay, 10 µl of purified fractions containing ~1 µg β-arrestin 2 were incubated for 10 min at 37°C in 5 µL kinase buffer (25 mM MOPS, pH 7.2, 12.5 mM β-glycerophosphate, 25 mM $MgCl_2$, 5 mM EGTA, 2 mM EDTA, 0.25 mM DTT) in absence or presence of 5 µL active MEK1 (EE, 0.025 µg/µL, Sigma Aldrich). Kinase reaction was started by adding 5 µL ATP (250 µM) and was stopped by adding Laemmli buffer. β-arrestin 2 phosphorylation at Thr^{383} was analyzed by Western blotting using the purified anti-phospho-Thr^{383}-β-arrestin 2 antibody. For radioactive kinase assay, 10 µl of purified fractions containing ~1 µg YFP-β-arrestin 2 or 1 µg of non-activated, purified GST-tagged Erk2 (Sigma Aldrich) were incubated for 10 min at 37°C in 5 µL kinase buffer in presence of active MEK1 and [γ-^{32}P]-ATP (50 µM, 2 µCi/nmol). Proteins were separated by SDS-PAGE and stained with colloidal Coomassie. Gels were dried and exposed for autoradiography. Radioactive bands corresponding to β-arrestin 2 and Erk2 were excised and radioactivity was measured by β-scintillation counting.

Western blotting

Proteins, resolved onto 10% polyacrylamide gels, were transferred to Hybond C nitrocellulose membranes (GE Healthcare). Membranes were immunoblotted with primary antibodies (anti phospho-Thr^{202}/Tyr^{204}-Erk1/2, 1:1,000; anti Erk1/2, 1:1,000; anti-Flag, 1:1,000; Anti-GFP, 1:1,000; anti-Myc, 1:1,000; anti-phospho-Thr^{383}-β-arrestin 2, 1:5,000; anti-β-arrestin 2, 1:1,000; anti-pan arrestin, 1/1,000) and then with either anti-mouse or anti-rabbit horseradish peroxidase-conjugated secondary antibodies (1:5,000, GE Healthcare). Immunoreactivity was detected with an enhanced chemiluminescence method (ECL^{TM} plus detection reagent, Perkin Elmer). Immunoreactive bands were quantified by densitometry using the ImageJ software. In protein phosphorylation analyses, the amount of each phosphoprotein was normalized to the corresponding total protein signal.

ELISA

Quantification of cell surface expression of Myc-tagged 5-HT$_{2C}$ and 5-HT$_4$ receptors was performed by ELISA under permeabilized (Triton X-100 0.05%) *vs.* non-permeabilized conditions, as previously described *(43)*. Dilutions for primary antibodies were 1:2,000 (Anti-Myc) and 1:500 (anti-integrin β1). Dilutions for secondary antibodies were 1:5,000 (donkey anti-goat conjugated to HRP) and 1:8,000 (goat anti-mouse conjugated to HRP). Immunoreactive signal was detected with a M200 Infinite plate reader (Tecan), using the SuperSignal® ELISA Femto chromogenic substrate (Thermo Scientific). Control experiments were performed using cells transfected with empty vectors and values were normalized with respect to the total amount of protein.

BRET experiments

HEK-293 cells were transiently co-transfected with either pEYFP-N1-Myc-5-HT$_{2C}$ or pEYFP-N1-Myc-5-HT$_4$ plasmids and either pcDNA3-Rluc-βARR2 or pcDNA3-Rluc-βARR2^{T383A} or pcDNA3-Rluc-βARR2^{T383D} plasmids for β-arrestin 2 recruitment to receptors. For double brilliance β-arrestin 2 assays, they were co-transfected with either pRK5-Myc-5-HT$_{2C}$ or pRK5-Myc-5-HT$_4$ and either pCMV-Rluc8-βARR2-RGFP or pCMV-Rluc8-

βARR2^{T383A}-RGFP or pCMV-Rluc8-βARR2^{T383D}-RGFP. Cells were grown in 96-well micro-plates (6×10^4 cells/well) for 48 h and starved of serum for 6 h. Cells were washed once with PBS and Coelenterazine H (Sigma-Aldrich) was added at a final concentration of 5 μM for 10 min. Cells were then challenged with 5-HT for 30 min. BRET readings were performed using a Mithras LB940 multimode microplate reader (Berthold Technologies) allowing sequential integration of luminescence with three filter settings: Rluc filter, 485 ± 10 nm; YFP filter, 530 ± 12.5 nm; RGFP filter, 515 ± 10 nm. Emission signals at 530 nm or 515 nm were divided by emission signals at 485 nm. The difference between this emission ratio obtained with donor and acceptor co-expressed or fused and that obtained with the donor protein expressed alone was defined as the BRET ratio. Results are expressed in milliBRET units corresponding to the BRET ratio multiplied by 1,000.

Docking

Modeling of the receptor/ß-arrestin/Erk module was made using the PRIOR method, and the PDB structures and methodology indicated in *(31)*. Structural images were made using Pymol.

Statistics

Statistical analyses were performed using Prism (v. 6.0, GraphPad Software Inc.). Unpaired t test and one-way ANOVA followed by Newman Keuls test were performed to compare two values and for multiple comparisons, respectively.

Information regarding statistical reporting

For each graph, the number of biological replicates (independent experiments performed on different sets of cultured cells) and significance of observed differences are indicated in the figure legend. The different levels of statistical significance are encoded with symbols (*, **,

***,) directly on the histograms and explained in the figure legends. The statistical tests and software used are indicated in "Materials and Methods section (page 20).

MS peptide identification probabilities were performed using the Mascot algorithm. Mascot search was performed using parameters described in the Material and methods section. Mascot score represents -10*LOG10(Pvalue), where Pvalue is the absolute probability of peptide wrong assignment.

ACKNOWLEDGMENTS

Funding: This work was supported by grants from la Fondation pour la Recherche Médicale (Contract Equipe FRM 2009), ANR (Contract n° ANR-2011-1619 01), CNRS, INSERM and University of Montpellier to PM and FV, and from ANR (Contract n° ANR-2011-1619 01), INRA and Université de Tours to ER, AP and PC. Mass spectrometry experiments were carried out using facilities of the Functional Proteomic Platform of Montpellier Languedoc-Roussillon, and BRET experiments using facilities of Arpege pharmacological screening platform. The authors wish to thank Cisbio Bioassays for the generation of the anti-phospho-Thr^{383}-β-arrestin 2 antibody.

Competing interests: The authors declare that they have no conflict of interest

REFERENCES

1. S. K. Shenoy, R. J. Lefkowitz, beta-Arrestin-mediated receptor trafficking and signal transduction. *Trends in pharmacological sciences* **32**, 521-533 (2011).
2. R. J. Lefkowitz, S. K. Shenoy, Transduction of receptor signals by beta-arrestins. *Science* **308**, 512-517 (2005).
3. C. Latapy, J. M. Beaulieu, beta-Arrestins in the central nervous system. *Progress in molecular biology and translational science* **118**, 267-295 (2013).

4. J. M. Beaulieu, R. R. Gainetdinov, M. G. Caron, The Akt-GSK-3 signaling cascade in the actions of dopamine. *Trends in pharmacological sciences* **28**, 166-172 (2007).

5. E. Reiter, R. J. Lefkowitz, GRKs and beta-arrestins: roles in receptor silencing, trafficking and signaling. *Trends Endocrinol Metab* **17**, 159-165 (2006).

6. K. A. DeFea, J. Zalevsky, M. S. Thoma, O. Dery, R. D. Mullins, N. W. Bunnett, beta-arrestin-dependent endocytosis of proteinase-activated receptor 2 is required for intracellular targeting of activated ERK1/2. *J Cell Biol* **148**, 1267-1281 (2000).

7. L. M. Luttrell, F. L. Roudabush, E. W. Choy, W. E. Miller, M. E. Field, K. L. Pierce, R. J. Lefkowitz, Activation and targeting of extracellular signal-regulated kinases by beta-arrestin scaffolds. *Proceedings of the National Academy of Sciences of the United States of America* **98**, 2449-2454 (2001).

8. S. Ahn, S. K. Shenoy, H. Wei, R. J. Lefkowitz, Differential kinetic and spatial patterns of beta-arrestin and G protein-mediated ERK activation by the angiotensin II receptor. *The Journal of biological chemistry* **279**, 35518-35525 (2004).

9. S. K. Shenoy, M. T. Drake, C. D. Nelson, D. A. Houtz, K. Xiao, S. Madabushi, E. Reiter, R. T. Premont, O. Lichtarge, R. J. Lefkowitz, beta-arrestin-dependent, G protein-independent ERK1/2 activation by the beta2 adrenergic receptor. *The Journal of biological chemistry* **281**, 1261-1273 (2006).

10. M. Labasque, E. Reiter, C. Becamel, J. Bockaert, P. Marin, Physical interaction of calmodulin with the 5-hydroxytryptamine2C receptor C-terminus is essential for G protein-independent, arrestin-dependent receptor signaling. *Mol Biol Cell* **19**, 4640-4650 (2008).

11. G. Barthet, B. Framery, F. Gaven, L. Pellissier, E. Reiter, S. Claeysen, J. Bockaert, A. Dumuis, 5-hydroxytryptamine 4 receptor activation of the extracellular signal-regulated kinase pathway depends on Src activation but not on G protein or beta-arrestin signaling. *Mol Biol Cell* **18**, 1979-1991 (2007).

12. H. Zheng, H. H. Loh, P. Y. Law, Beta-arrestin-dependent mu-opioid receptor-activated extracellular signal-regulated kinases (ERKs) Translocate to Nucleus in Contrast to G protein-dependent ERK activation. *Molecular pharmacology* **73**, 178-190 (2008).

13. A. K. Shukla, K. Xiao, R. J. Lefkowitz, Emerging paradigms of beta-arrestin-dependent seven transmembrane receptor signaling. *Trends Biochem Sci* **36**, 457-469 (2011).

14. F. T. Lin, K. M. Krueger, H. E. Kendall, Y. Daaka, Z. L. Fredericks, J. A. Pitcher, R. J. Lefkowitz, Clathrin-mediated endocytosis of the beta-adrenergic receptor is regulated by phosphorylation/dephosphorylation of beta-arrestin1. *The Journal of biological chemistry* **272**, 31051-31057 (1997).

15. G. Barthet, G. Carrat, E. Cassier, B. Barker, F. Gaven, M. Pillot, B. Framery, L. P. Pellissier, J. Augier, D. S. Kang, S. Claeysen, E. Reiter, J. L. Baneres, J. L. Benovic, P. Marin, J. Bockaert, A. Dumuis, Beta-arrestin1 phosphorylation by GRK5 regulates G protein-independent 5-HT4 receptor signalling. *EMBO J* **28**, 2706-2718 (2009).

16. F. T. Lin, W. E. Miller, L. M. Luttrell, R. J. Lefkowitz, Feedback regulation of beta-arrestin1 function by extracellular signal-regulated kinases. *The Journal of biological chemistry* **274**, 15971-15974 (1999).

17. F. T. Lin, W. Chen, S. Shenoy, M. Cong, S. T. Exum, R. J. Lefkowitz, Phosphorylation of beta-arrestin2 regulates its function in internalization of beta(2)-adrenergic receptors. *Biochemistry* **41**, 10692-10699 (2002).

18. J. S. Paradis, S. Ly, E. Blondel-Tepaz, J. A. Galan, A. Beautrait, M. G. Scott, H. Enslen, S. Marullo, P. P. Roux, M. Bouvier, Receptor sequestration in response to beta-arrestin-2 phosphorylation by ERK1/2 governs steady-state levels of GPCR cell-surface expression. *Proceedings of the National Academy of Sciences of the United States of America* **112**, E5160-5168 (2015).

19. Y. M. Kim, L. S. Barak, M. G. Caron, J. L. Benovic, Regulation of arrestin-3 phosphorylation by casein kinase II. *The Journal of biological chemistry* **277**, 16837-16846 (2002).

20. E. Khoury, L. Nikolajev, M. Simaan, Y. Namkung, S. A. Laporte, Differential regulation of endosomal GPCR/beta-arrestin complexes and trafficking by MAPK. *The Journal of biological chemistry* **289**, 23302-23317 (2014).

21. C. Pighi, T. L. Gu, I. Dalai, S. Barbi, C. Parolini, A. Bertolaso, S. Pedron, A. Parisi, J. Ren, D. Cecconi, M. Chilosi, F. Menestrina, A. Zamo, Phospho-proteomic analysis of mantle cell lymphoma cells suggests a pro-survival role of B-cell receptor signaling. *Cell Oncol (Dordr)* **34**, 141-153 (2011).

22. K. Sharma, R. C. D'Souza, S. Tyanova, C. Schaab, J. R. Wisniewski, J. Cox, M. Mann, Ultradeep human phosphoproteome reveals a distinct regulatory nature of Tyr and Ser/Thr-based signaling. *Cell Rep* **8**, 1583-1594 (2014).

23. B. A. Ballif, G. R. Carey, S. R. Sunyaev, S. P. Gygi, Large-scale identification and evolution indexing of tyrosine phosphorylation sites from murine brain. *Journal of proteome research* **7**, 311-318 (2008).

24. J. Villen, S. A. Beausoleil, S. A. Gerber, S. P. Gygi, Large-scale phosphorylation analysis of mouse liver. *Proceedings of the National Academy of Sciences of the United States of America* **104**, 1488-1493 (2007).

25. C. Choudhary, J. V. Olsen, C. Brandts, J. Cox, P. N. Reddy, F. D. Bohmer, V. Gerke, D. E. Schmidt-Arras, W. E. Berdel, C. Muller-Tidow, M. Mann, H. Serve, Mislocalized activation of oncogenic RTKs switches downstream signaling outcomes. *Molecular cell* **36**, 326-339 (2009).

26. C. Jorgensen, A. Sherman, G. I. Chen, A. Pasculescu, A. Poliakov, M. Hsiung, B. Larsen, D. G. Wilkinson, R. Linding, T. Pawson, Cell-specific information processing in segregating populations of Eph receptor ephrin-expressing cells. *Science* **326**, 1502-1509 (2009).

27. Y. Xue, J. Ren, X. Gao, C. Jin, L. Wen, X. Yao, GPS 2.0, a Tool to Predict Kinase-specific Phosphorylation Sites in Hierarchy. *Mol Cell Proteomics* **7**, 1598-1608 (2008).

28. M. A. Pagano, G. Poletto, G. Di Maira, G. Cozza, M. Ruzzene, S. Sarno, J. Bain, M. Elliott, S. Moro, G. Zagotto, F. Meggio, L. A. Pinna, Tetrabromocinnamic acid (TBCA) and related compounds represent a new class of specific protein kinase CK2 inhibitors. *Chembiochem* **8**, 129-139 (2007).

29. K. Xiao, S. K. Shenoy, K. Nobles, R. J. Lefkowitz, Activation-dependent conformational changes in {beta}-arrestin 2. *The Journal of biological chemistry* **279**, 55744-55753 (2004).

30. V. V. Gurevich, E. V. Gurevich, The new face of active receptor bound arrestin attracts new partners. *Structure* **11**, 1037-1042 (2003).

31. T. Bourquard, F. Landomiel, E. Reiter, P. Crepieux, D. W. Ritchie, J. Aze, A. Poupon, Unraveling the molecular architecture of a G protein-coupled receptor/beta-arrestin/Erk module complex. *Sci Rep* **5**, 10760 (2015).

32. V. V. Gurevich, E. V. Gurevich, Extensive shape shifting underlies functional versatility of arrestins. *Current opinion in cell biology* **27**, 1-9 (2014).

33. M. Kamal, M. Marquez, V. Vauthier, A. Leloire, P. Froguel, R. Jockers, C. Couturier, Improved donor/acceptor BRET couples for monitoring beta-arrestin recruitment to G protein-coupled receptors. *Biotechnology journal* **4**, 1337-1344 (2009).

34. P. G. Charest, S. Terrillon, M. Bouvier, Monitoring agonist-promoted conformational changes of beta-arrestin in living cells by intramolecular BRET. *EMBO Rep* **6**, 334-340 (2005).

35. E. Kara, P. Crepieux, C. Gauthier, N. Martinat, V. Piketty, F. Guillou, E. Reiter, A phosphorylation cluster of five serine and threonine residues in the C-terminus of the follicle-stimulating hormone receptor is important for desensitization but not for beta-arrestin-mediated ERK activation. *Mol Endocrinol* **20**, 3014-3026 (2006).

694 36. Y. Sun, Z. Cheng, L. Ma, G. Pei, Beta-arrestin2 is critically involved in CXCR4-
695 mediated chemotaxis, and this is mediated by its enhancement of p38 MAPK
696 activation. *The Journal of biological chemistry* **277**, 49212-49219 (2002).

697 37. K. Xiao, D. B. McClatchy, A. K. Shukla, Y. Zhao, M. Chen, S. K. Shenoy, J. R.
698 Yates, 3rd, R. J. Lefkowitz, Functional specialization of beta-arrestin interactions
699 revealed by proteomic analysis. *Proceedings of the National Academy of Sciences of*
700 *the United States of America* **104**, 12011-12016 (2007).

701 38. M. Han, V. V. Gurevich, S. A. Vishnivetskiy, P. B. Sigler, C. Schubert, Crystal
702 structure of beta-arrestin at 1.9 A: possible mechanism of receptor binding and
703 membrane Translocation. *Structure* **9**, 869-880 (2001).

704 39. X. Zhan, L. E. Gimenez, V. V. Gurevich, B. W. Spiller, Crystal structure of arrestin-3
705 reveals the basis of the difference in receptor binding between two non-visual
706 subtypes. *J Mol Biol* **406**, 467-478 (2011).

707 40. A. K. Shukla, A. Manglik, A. C. Kruse, K. Xiao, R. I. Reis, W. C. Tseng, D. P. Staus,
708 D. Hilger, S. Uysal, L. Y. Huang, M. Paduch, P. Tripathi-Shukla, A. Koide, S. Koide,
709 W. I. Weis, A. A. Kossiakoff, B. K. Kobilka, R. J. Lefkowitz, Structure of active beta-
710 arrestin-1 bound to a G-protein-coupled receptor phosphopeptide. *Nature* **497**, 137-
711 141 (2013).

712 41. E. D. Por, R. Gomez, A. N. Akopian, N. A. Jeske, Phosphorylation regulates TRPV1
713 association with beta-arrestin-2. *The Biochemical journal* **451**, 101-109 (2013).

714 42. R. J. Lefkowitz, K. L. Pierce, L. M. Luttrell, Dancing with different partners: protein
715 kinase a phosphorylation of seven membrane-spanning receptors regulates their G
716 protein-coupling specificity. *Mol Pharmacol* **62**, 971-974 (2002).

717 43. B. Chanrion, C. Mannoury la Cour, S. Gavarini, M. Seimandi, L. Vincent, J. F. Pujol,
718 J. Bockaert, P. Marin, M. J. Millan, Inverse agonist and neutral antagonist actions of
719 antidepressants at recombinant and native 5-hydroxytryptamine2C receptors:

differential modulation of cell surface expression and signal transduction. *Molecular pharmacology* **73**, 748-757 (2008).

44. L. P. Pellissier, G. Barthet, F. Gaven, E. Cassier, E. Trinquet, J. P. Pin, P. Marin, A. Dumuis, J. Bockaert, J. L. Baneres, S. Claeysen, G protein activation by serotonin type 4 receptor dimers: evidence that turning on two protomers is more efficient. *The Journal of biological chemistry* **286**, 9985-9997 (2011).

45. T. Tranchant, G. Durand, C. Gauthier, P. Crepieux, A. Ulloa-Aguirre, D. Royere, E. Reiter, Preferential beta-arrestin signalling at low receptor density revealed by functional characterization of the human FSH receptor A189 V mutation. *Mol Cell Endocrinol* **331**, 109-118 (2011).

46. F. Dubois, F. Vandermoere, A. l. Gernez, J. Murphy, R. Toth, S. Chen, K. M. Geraghty, N. A. Morrice, C. MacKintosh, Differential 14-3-3 affinity capture reveals new downstream targets of phosphatidylinositol 3-kinase signaling. *Mol. Cell Proteomics* **8**, 2487-2499 (2009).

47. S. Ahn, H. Wei, T. R. Garrison, R. J. Lefkowitz, Reciprocal regulation of angiotensin receptor-activated extracellular signal-regulated kinases by beta-arrestins 1 and 2. *The Journal of biological chemistry* **279**, 7807-7811 (2004).

FIGURE LEGENDS

Figure 1. 5-HT_{2C} and 5-HT_4 receptor stimulation promotes β-arrestin-2 phosphorylation in HEK-293 cells. A. Ribbon diagram of rat β-arrestin 2 showing the position of phosphorylated residues identified by LS-MS/MS. **B.** Representative extracted ion chromatograms of the EIDIPVDTNLIEFDTNYAp^{383}TDDDIVFEDFAR peptide from YFP-tagged β-arrestin 2 in cells expressing 5-HT_{2C} or 5-HT_4 receptor and challenged with vehicle (Basal) or 5-HT (1 and 10 µM, respectively) for 5 or 30 min. Two other independent experiments performed on different sets of cultured cells yielded similar results. The histogram represents the means ± SEM of ion signal intensities of the peptide obtained in the three experiments. **C.** 5-HT_{2C} or 5-HT_4 receptor expressing cells were treated as in (**B**). Erk1,2 activation and Thr^{383} phosphorylation were assessed by Western blotting using the anti-phospho-Thr^{202}/Tyr^{204}-Erk1/2 and the anti-phospho-Thr^{383} β-arrestin 2 antibody, respectively. The histogram shows the means ± SEM of the anti-phospho-Thr^{383} β-arrestin 2 immunoreactive signals (expressed in arbitrary unit) obtained in three independent experiments performed on different sets of cultured cells. One-way ANOVA: (B) $F(5,12)=7.544$, $p=0.0020$; (C) $F(4,10) = 4.417$, $P= 0.0259$. * $p<0.05$ *vs.* corresponding vehicle.

Figure 1 - Figure supplement 1. Purification of YFP-β-arrestin 1 and YFP-β-arrestin 2 co-expressed with 5-HT_{2C} or 5-HT_4 receptor in HEK-293 cells. YFP-β-arrestin 1 (A) and YFP-β-arrestin 2 (B) co-expressed with Myc-tagged 5-HT_{2C} or 5-HT_4 receptor were immunoprecipitated using GFP Trap beads and detected by Western blotting using an anti-GFP antibody (10% of IP) and by colloidal Coomassie blue staining (90% of IP). Receptor expression and functionality were assessed by immunoblotting using an anti-Myc antibody, and by sequential immunoblotting with the antibody recognizing phospho-Thr^{202}/Tyr^{204}-Erk1/2 and total Erk1/2. Immunoblots and gels representative of four independent experiments are illustrated. Note that 5-HT_4 receptor immunoreactivity was detected at molecular weights corresponding to receptor monomer and dimer.

Figure 1 - Figure supplement 2. Sequence coverage of β-arrestin 1 and β-arrestin 2 obtained by LC-MS/MS. The sequence covered by LC-MS/MS analysis is highlighted in red. Identified phosphorylated residues in β-arrestin 1 (Thr^{374}) and β-arrestin 2 (Thr^{178}, Ser^{194}, $Ser^{267/268}$, Ser^{281}, Ser^{361} and Thr^{383}) and their positions are highlighted in blue.

Figure 1 - Figure supplement 3. Tandem mass spectra of EVPESETPVDpT^{374}NLIELDT NDDDIVFEDFAR, CPVAQLEQDDQVSPp(S^{267}S^{268})TFCK and EIDIPVDTNLIEFD TNYApT^{383}DDDIVFEDFAR phosphorylated peptides identified from YFP-tagged β-arrestin 1 and β-arrestin 2 transiently co-expressed with 5-HT$_{2C}$ receptor in HEK-293 cells and immunoprecipitated using the GFP Trap kit. For each identified phosphorylated peptide, MS/MS spectra that yielded the highest Mascot score, matched b and y ions, peptide sequence and position of the phosphorylated residue in the full-length protein are illustrated.

Figure 1 - Figure supplement 4. Tandem mass spectra of HFLMpS^{194}DRR, KVQFAPE pT^{178}PGPQPSAETTR and PHDHITLPRPQpS^{361}APR phosphorylated peptides identified from YFP-tagged β-arrestin 1 and β-arrestin 2 transiently co-expressed with 5-HT$_{2C}$ receptor in HEK-293 cells and immunoprecipitated using the GFP Trap kit. For each identified phosphorylated peptide, MS/MS spectra that yielded the highest Mascot score, matched b and y ions, peptide sequence and position of the phosphorylated residue in the full-length protein are illustrated.

Figure 1 - Figure supplement 5. Tandem mass spectra of VQFAPEpT^{178}PGPQPSAET TR, VYTITPLLpS^{281}DNR, VYTITPLLpS^{281}DNREK phosphorylated peptides identified from YFP-tagged β-arrestin 1 and β-arrestin 2 transiently co-expressed with 5-HT$_{2C}$ receptor in HEK-293 cells and immunoprecipitated using the GFP Trap kit. For each identified phosphorylated peptide, MS/MS spectra that yielded the highest Mascot score,

matched b and y ions, peptide sequence and position of the phosphorylated residue in the full-length protein are illustrated.

Figure 1 - Source data 1. List of phosphorylated peptides identified from purified β-arrestin 1 and β-arrestin 2 by nano-LC-MS/MS. Quantitative data were used to build histogram in Figure 1B. Phosphorylated peptides were analyzed by nano-LC-MS/MS using multistage activation on the neutral loss of phosphoric acid. For each peptide, the position of modified residue(s) in the protein sequence, experimental and theoretical masses, mass deviation, charge, Mascot score and corresponding P value are indicated. The phosphorylation index (phosphorylated peptide MS signal intensity / phosphorylated peptide MS signal intensity + non-phosphorylated peptide MS signal intensity) in cells expressing or not 5-HT_{2C} or 5-HT_4 receptor and treated with vehicle or 5-HT was also calculated for each phosphorylated peptide identified. ND: not detected. Results of one-way ANOVA for the EIDIPVDTNLIEFDTNYApTDDDIVFEDFAR peptide: $F(5,12) = 7.544$, $p = 0.020$. * $p<0.05$ *vs.* vehicle.

Figure 1 - Source data 2.

This file contains raw values used to build Figure 1C.

Figure 2. Role of MEK in the phosphorylation of β-arrestin 2 at Thr^{383} elicited by 5-HT_{2C} receptor stimulation. A. Mechanistic model of assembly of the 5-HT_{2C} receptor/β-arrestin 2/Erk module. Color code: receptor in orange, MEK in green, β-arrestin 2 core in pale cyan and C-tail in cyan (the regions 351-384 and 394-419, which are not visible in 3D structure are represented by dashed lines, the region 385-393 is represented by spheres), Erk in dark red, Raf-1 RBD domain in pink. In this model we hypothesize that Thr^{383} phosphorylation by MEK takes place within the assembled receptor/β-arrestin/Raf/MEK complex and results in a movement of β-arrestin 2 unfolded 350-393 segment away from the

first β-strand of β-arrestin, leaving space for further interaction with the receptor C-terminal domain (orange spheres) and recruitment of Erk, and its subsequent phosphorylation by MEK. For the clarity of the figure, the extremity of the β-arrestin C-tail is represented by spheres even in its unfolded state, although the real 3D structure is unknown. **B.** Representative extracted ion chromatograms of the peptide in cells expressing 5-HT_{2C} receptor, pretreated with either vehicle (control) or FR180204 (10 µM for 18 h) or U0126 (5 µM for 30 min) or coexpressing MEK1 dominant-negative mutant (MEK1DN), and challenged with vehicle (Basal) or 5-HT (1 µM) for 30 min. The histogram represents the means ± SEM of the corresponding ion signal intensities (normalized to values in 5-HT-stimulated cells in Control condition) obtained in three independent experiments. One-way ANOVA: $F(8,18) = 15.69$, $p<0.0001$. *** $p<0.001$ *vs.* corresponding basal value. **C.** YFP-tagged β-arrestin2 (wild-type or Thr^{383}Ala mutant) purified from transfected HEK-293 cells was incubated with active MEK1 for 15 min at 37°C. When indicated, U0126 (5 µM) was included in the incubation medium. Thr^{383} phosphorylation was assessed by sequential immunoblotting with the antibody raised against phospho-Thr^{383} β-arrestin 2 and the anti-β-arrestin 2 antibody. Means ± SEM of results from 4 independent experiments are shown on the histogram. n.d.: not detectable. One-way ANOVA: $F(2,9) = 352.2$, $p<0.0001$. *** $p<0.001$ *vs.* immunoreactive signal in absence of MEK; §§§ $p<0.001$ *vs.* corresponding condition in absence of U0126.

Figure 2 – Figure supplement 1. Thr^{383} phosphorylation is not mediated by casein kinase 2. **A.** Representative extracted ion chromatograms of the EIDIPVDTNLIEFDTNYAp^{383}TDDDIVFEDFAR peptide from YFP-tagged β-arrestin 2 in cells expressing 5-HT_{2C} receptor and challenged with vehicle (Basal) or 1 µM 5-HT for 30 min in absence or presence of TBCA (1 µM, added 15 min before the onset of 5-HT treatment). Two other independent experiments performed on different sets of cultured cells yielded similar results. **B.** The histogram represents the means ± SEM of ion signal intensities of the peptide (normalized to values in 5-HT-stimulated cells) obtained in the three experiments. One-way ANOVA $F(3,8) = 6.762$, $p=0.013$. * $p<0.05$ *vs.* corresponding vehicle.

Figure 2 - Figure supplement 2. Impact of MEK and Erk1/2 pharmacological inhibitors and of co-expression of MEK dominant-negative mutant on 5-HT_{2C} receptor-operated Erk1/2 and Elk1 phosphorylation. A. Cells expressing 5-HT_{2C} receptor were pretreated with vehicle or U0126 (5 μM for 30 min) or FR180204 (10 μM for 18 h) and then exposed to vehicle or 5-HT (1 μM) for 5 min. When indicated, a dominant-negative mutant of MEK (MEKDN) was co-expressed by 5-HT_{2C} receptor. Erk1/2 activation was assessed by sequential immunoblotting with the antibody recognizing phospho-Thr^{202}/Tyr^{204}-Erk1/2 and total Erk1/2. Immunoblots representative of three independent experiments are illustrated. Note that FR180184 did not affect 5-HT_{2C} receptor-operated Erk1/2 phosphorylation, indicating that it does not inhibit MEK. **B.** The impact of MEK and Erk1/2 inhibitors on phosphorylation of the Erk1/2 substrate Elk1 was assessed by sequential immunoblotting with the antibody recognizing phospho-Elk1 and total Elk1. Immunoblots representative of two independent experiments are illustrated.

Figure 2 - Figure supplement 3: *In vitro* phosphorylation of β-arrestin-2 versus Erk2 by MEK1. YFP-tagged β-arrestin 2 (wild-type or Thr^{383}Ala mutant) purified from transfected HEK-293 cells or purified non-activated Erk2 (~1 μg each) were incubated with active MEK1 in presence of [γ-^{32}P]-ATP (2 μCi/nmol) for 10 min at 37°C. Proteins were separated by SDS-PAGE and stained with Coomassie colloidal blue (top image) and ^{32}P incorporation into the different substrates was monitored by autoradiography (bottom image). The data in the histogram, expressed in nmol/min/mg enzyme, represent the means ± SD of ^{32}P incorporation into β-arrestin-2 and Erk2 protein bands in the corresponding experiment after radioactive background subtraction for each lane.

Figure 2 - Source data 1.

This file contains raw values used to build Figure 2B and Figure 2C.

Figure 2 – Figure Supplement 1 - Source data 1.

This file contains raw values used to build Figure 2 - Figure Supplement 1

Figure 2 – Figure Supplement 3 - Source data 1.

This file contains raw values used to build Figure 2 - Figure Supplement 3

Figure 3. Thr^{383} phosphorylation underlies β-arrestin 2 conformational rearrangement elicited by 5-HT$_{2C}$ receptor stimulation. A, B. Translocation of wild type (WT), T^{383}A and T^{383}D Rluc-β-arrestin-2 to Myc-5-HT$_{2C}$-YFP (**A**) or Myc-5-HT$_4$-YFP (**B**) receptors in cells treated with either vehicle (Basal) or 1 or 10 µM 5-HT, respectively, was measured by BRET. Data represent the mean ± SEM of values obtained in three independent experiments and were normalized to the BRET signals measured in 5-HT stimulated cells expressing WT Rluc β-arrestin 2. **C, D**. Cell surface expression of receptors was measured in the same experimental condition by ELISA using anti-Myc antibody. Data are the mean ± SEM of values obtained in three independent experiments. They were normalized to total receptor expression level and are expressed in % of basal receptor level at the cell surface in cells expressing WT β-arrestin 2. **E, F.** Conformational arrangement of WT, T^{383}A and T^{383}D double brilliance Rluc8-β-arrestin 2-RGFP elicited by 5-HT$_{2C}$ and 5-HT$_4$ receptor stimulation by 5-HT (1 and 10 µM, respectively). Equivalent expression of each BRET sensor was verified by ELISA. Data represent the mean ± SEM of values obtained in three independent experiments and were normalized to the basal intra-molecular BRET signal in cells expressing WT Rluc8-β-arrestin 2-RGFP. One-way ANOVA: A, $F(5,12)=10.75$, $p=0.0004$; B, $F(5,12)=320.9$, $p<0.001$; C, $F(6,14)=10.82$, $p<0.0001$; D, $F(6,14)=48.52$, $p<0.0001$; E, $F(5,12)=5.136$, $p=0.0095$; F, $F(5,12)=6.436$, $p=0.004$. * $p<0.05$, ** $p<0.01$ *** $p<0.001$ *vs.* corresponding basal.

Figure 3 - Source data 1.

This file contains raw values used to build Figure 3.

Figure 4. Phosphorylation of β-arrestin 2 at Thr^{383} is a necessary step in Erk1/2 recruitment to β-arrestin 2 and engagement of Erk signaling by 5-HT_{2C} receptor. A, B. Recruitment of Erk1/2 to WT, $T^{383}A$ and $T^{383}D$ YFP-β-arrestin 2 in cells expressing 5-HT_{2C} or 5-HT_4 receptor and exposed or not to 5-HT (1 and 10 µM, respectively) was assessed by co-immunoprecipitation. Immunoblots representative of three independent experiments are illustrated. The histograms represent the means ± SEM of Erk1/2 immunoreactive signals in immunoprecipitates, assessed by densitometric analysis, obtained in the three experiments. They were normalized to the amount of YFP-β-arrestin 2 immunoprecipitates and expressed in % of basal level measured in cells expressing WT β-arrestin 2. * $p<0.05$ *vs.* basal value in cells expressing WT β-arrestin 2. **C, D.** Erk1/2 activation in cells co-expressing 5-HT_{2C} or 5-HT_4 receptor and either WT, or $T^{383}A$ and or $T^{383}D$ YFP-β-arrestin 2 and exposed or not to 5-HT (1 and 10 µM, respectively) for 5 or 30 min was assessed by sequential immunoblotting with the antibody recognizing phospho-Thr^{202}/Tyr^{204}-Erk1/2 and total Erk1/2. Immunoblots representative of three independent experiments are illustrated. The histograms represent the means ± SEM of values (normalized to the level of phosphorylated Erk1/2 in cells expressing WT β-arrestin 2 and exposed to 5-HT for 5 min) obtained in the three experiments. One-Way ANOVA: A, $F(5,12)=4.305$, $p=0.00178$; B, $F(5,12)=0.977$, $p=0.47$; C, $F(8,18)=11.78$, $p<0001$; D, $F(8,18)=4.998$, $p=0.0022$. * $p<0.05$, ** $p<0.01$ *vs.* corresponding value in cells expressing WT β-arrestin 2.

Figure 4 - Figure supplement 1. Role of MEK in Erk recruitment to β-arrestin 2. HEK-293 cells co-expressing YFP-β-arrestin 2 and 5-HT_{2C} receptor were treated for 30 min with vehicle or 1 µM 5-HT in absence or presence of 5 µM U0126 (added 15 min before the onset of 5-HT application). Recruitment of Erk1/2 to β-arrestin 2 was assessed by co-

immunoprecipitation. Immunoblots representative of three independent experiments are illustrated. The histogram represents the means ± SEM of Erk1/2 immunoreactive signals in immunoprecipitates normalized to the amount of YFP-β-arrestin 2 immunoprecipitates, obtained in the three experiments. They were expressed in % of Erk immunoreactive signal measured in 5-HT-stimulated cells. One-way ANOVA: $F(4,10) = 12,21$, $p = 0.0007$. ** $p<0.01$ *vs.* vehicle.

Figure 4 - Source data 1.

This file contains raw values used to build Figure 4.

Figure 4 - Figure supplement 1 - Source data 1.

This file contains raw values used to build Figure 4 - Figure supplement 1.

Figure 5. Phosphorylation of β-arrestin 2 at Thr^{383} underlies β-arrestin-dependent engagement of Erk1/2 signaling by FSH, β-adrenergic and CXCR4 receptors. Erk1/2 activation elicited by stimulation for the indicated times of transiently expressed FSH receptor (FSH, 3.3 nM), native β-adrenergic (isoproterenol 1 μM) and CXCR4 receptors (CXCL12, 10 nM) in cells transfected with control siRNA or β-arrestin 2 siRNA (**A-C**) and in cells coexpressing WT or $T^{383}A$ β-arrestin 2 (**D-F**). Erk1/2 activation was assessed by sequential immunoblotting with the antibody recognizing phospho-Thr^{202}/Tyr^{204}-Erk1/2 and total Erk1/2. Immunoblots representative of three independent experiments are illustrated. The histograms represent the means ± SEM of values (normalized to the level of phosphorylated Erk1/2 in cells exposed to agonist for 5 min) obtained in the three experiments. One way ANOVA: A, $F(5,12)=8.178$, $p=0.0014$; B, $F(5,12)=16.97$, $p<0.001$; C, $F(5,12)=20.22$, $p=<0.001$; D, $F(5,12)=7.710$, $p=0.0019$; E, $F(5,12)=29.76$, $p<0.0001$; $F(5,12)=8.695$, $p=.0.0012$. * $p<0.05$ and ** $p<0.01$ *vs.* corresponding value in control siRNA transfected cells or cells expressing WT β-arrestin 2.

Figure 5 - Figure supplement 1. **Down-regulation of β-arrestin 2 protein expression in HEK-293 cells using siRNA.** Cells were transfected with either control or β-arrestin 2 siRNA in absence (Mock, **A**) or presence (**B**) of the plasmid encoding FSH receptor. Cells were lysed 72 h after transfection and expression of β-arrestin 2 was measured by Western blotting. Equal loading was assessed by immunoblotting using a GAPDH antibody. Representative immunoblots of three independent experiments are illustrated. The histograms show the quantification of β-arrestin 2 immunoreactivity in the corresponding experiments. Data, expressed in % of value measured in cells transfected with control siRNA, are means ± SEM of results obtained in three independent experiments. Unpaired t-test, A, p=0.008 *vs.* control siRNA; B, p=0.0017 *vs.* control siRNA.

Figure 5 - Source data 1.

This file contains raw values used to build Figure 5.

Figure 5 -Figure supplement 1 - Source data 1.

This file contains raw values used to build Figure 5 - Figure supplement 1.

Figure 6. Schematic representation of the sequence of events proposed for β-arrestin-dependent Erk1/2 activation by GPCRs. β-arrestin, Raf and MEK are recruited to agonist-stimulated receptor, resulting in MEK activation. Active MEK phosphorylates β-arrestin 2 at Thr^{383}. This induces a movement of the β-arrestin 2 350-393 segment away from the first β-strand of β-arrestin, leaving space for its interaction with the C-terminal domain of the receptor. Erk then binds to the complex and is activated by MEK. The dash circles represent activated enzymes.

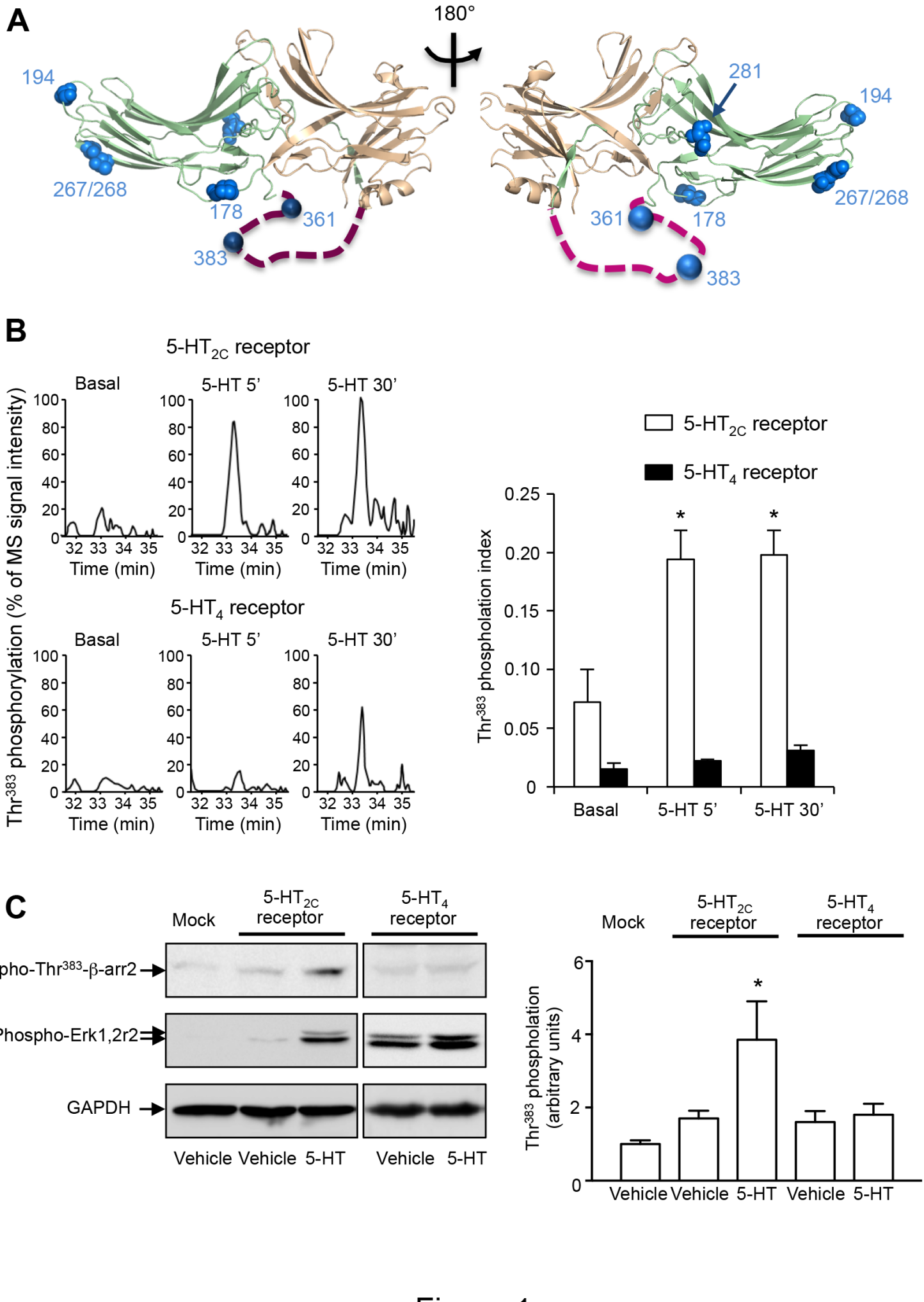
A
180°
194
267/268
178
361
383
281
194
267/268
361
178
383
B
5-HT2C receptor
Basal
5-HT 5'
5-HT 30'
Thr383 phosphorylation (% of MS signal intensity)
Time (min)
5-HT4 receptor
5-HT2C receptor
5-HT4 receptor
Thr383 phospholation index
Basal
5-HT 5'
5-HT 30'
C
Mock
5-HT2C receptor
5-HT4 receptor
Phospho-Thr383-β-arr2
Phospho-Erk1,2r2
GAPDH
Vehicle
Vehicle
5-HT
Vehicle
5-HT
Thr383 phospholation (arbitrary units)

Figure 1

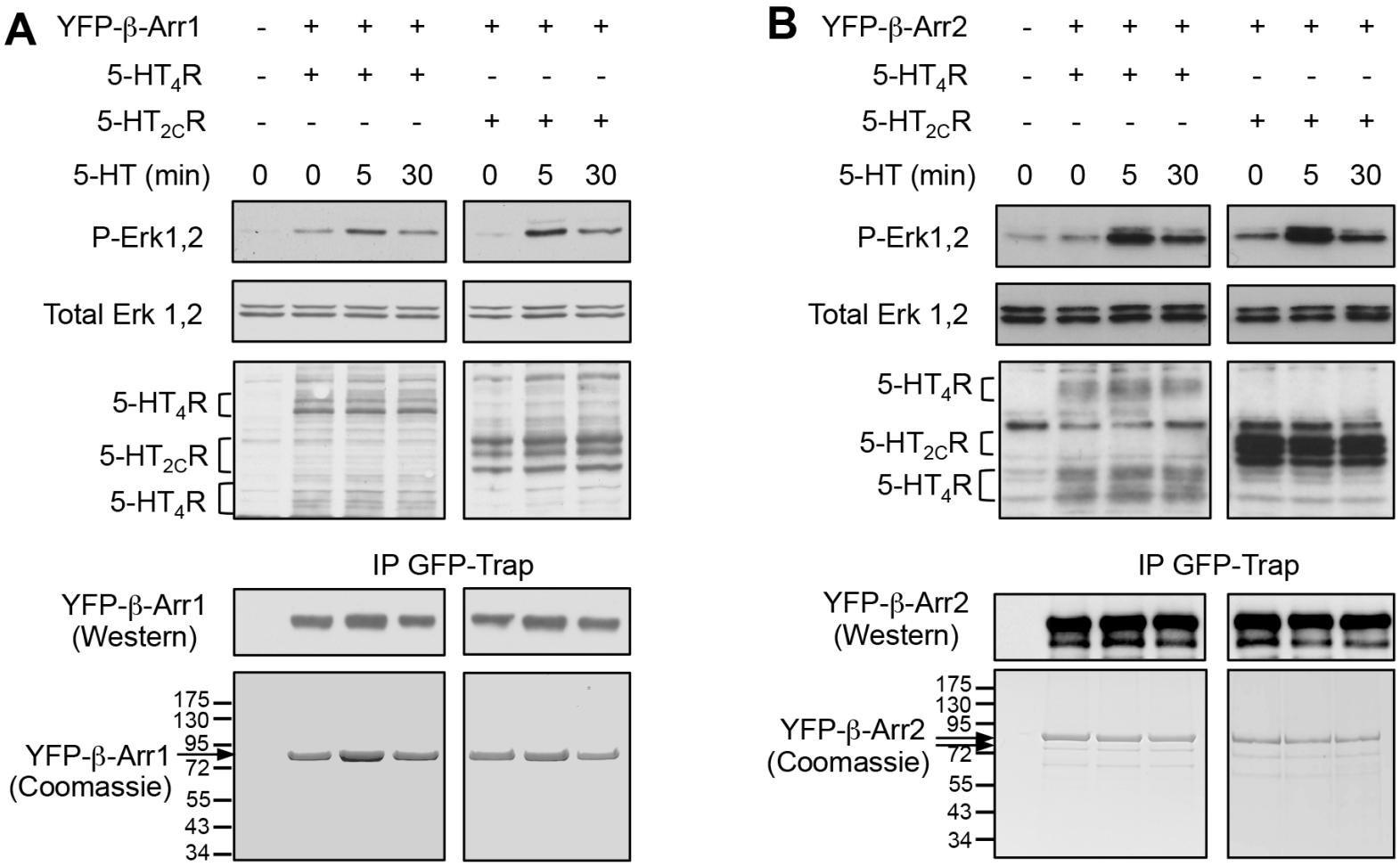

Figure 1 – Figure supplement 1

A β-arrestin 1 coverage: 88% (exp pvalue cut off 0.01)

```
1   MGDKGTRVFK KASPNGKLTV YLGKRDFVDH   IDLVDPVDGV VLVDPEYLKE
51  RRVYVTLTCA FRYGREDLDV LGLTFRKDLF   VANVQSFPPA PEDKKPLTRL
101 QERLIKKLGE HAYPFTFEIP PNLPCSVTLQ   PGPEDTGKAC GVDYEVKAFC
151 AENLEEKIHK RNSVRLVIRK VQYAPERPGP   QPTAETTRQF LMSDKPLHLE
201 ASLDKEIYYH GEPISVNVHV TNNTNKTVKK   IKISVRQYAD ICLFNTAQYK
251 CPVAMEEADD TVAPSSTFCK VYTLTPFLAN   NREKRGLALD GKLKHEDTNL
301 ASSTLLREGA NREILGIIVS YKVKVKLVVS   RGGLLGDLAS SDVAVELPFT
351 LMHPKPKEEP PHREVPESET PVDT[374]NLIELD TNDDDIVFED FARQRLKGMK
401 DDKDEEDDGT GSPHLNNR
```

B β-arrestin 2 coverage: 85% (exp pvalue cut off 0.01)

```
1   MGEKPGTRVF KKSSPNCKLT    VYLGKRDFVD   HLDKVDPVDG   VVLVDPDYLK
51  DRKVFVTLTC AFRYGREDLD    VLGLSFRKDL   FIATYQAFPP   MPNPPRPPTR
101 LQDRLLKKLG QHAHPFFFTI    PQNLPCSVTL   QPGPEDTGKA   CGVDFEIRAF
151 CAKSIEEKSH KRNSVRLIIR    KVQFAPET[178]PG PQPSAETTRH   FLMS[194]DRRS[198]LH
201 LEASLDKELY YHGEPLNVNV    HVTNNSAKTV   KKIRVSVRQY   ADICLFSTAQ
251 YKCPVAQLEQ DDQVSPS[267]S[268]TF CKVYTITPLL   S[281]DNREKRGLA LDGQLKHEDT
301 NLASSTIVKE GANKEVLGIL    VSYRVKVKLV   VSRGGDVSVE   LPFVLMHPKP
351 HDHITLPRPQ S[361]APREIDIPV   DTNLIEFDTN   YAT[383]DDDIVFE DFARLRLKGM
401 KDDDCDDQFC
```

Figure 1 - Figure Supplement 2

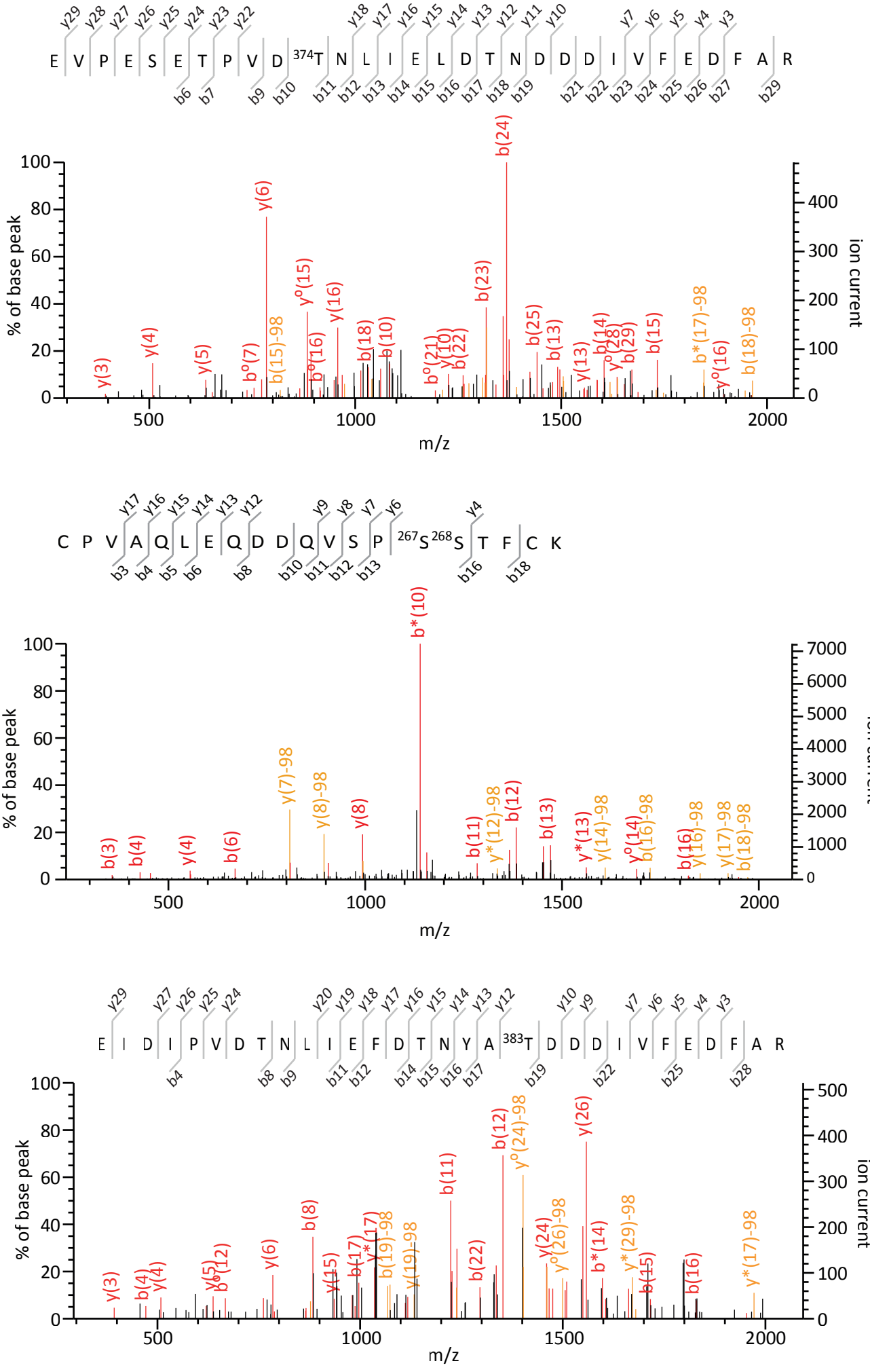

Figure 1 - Figure supplement 3

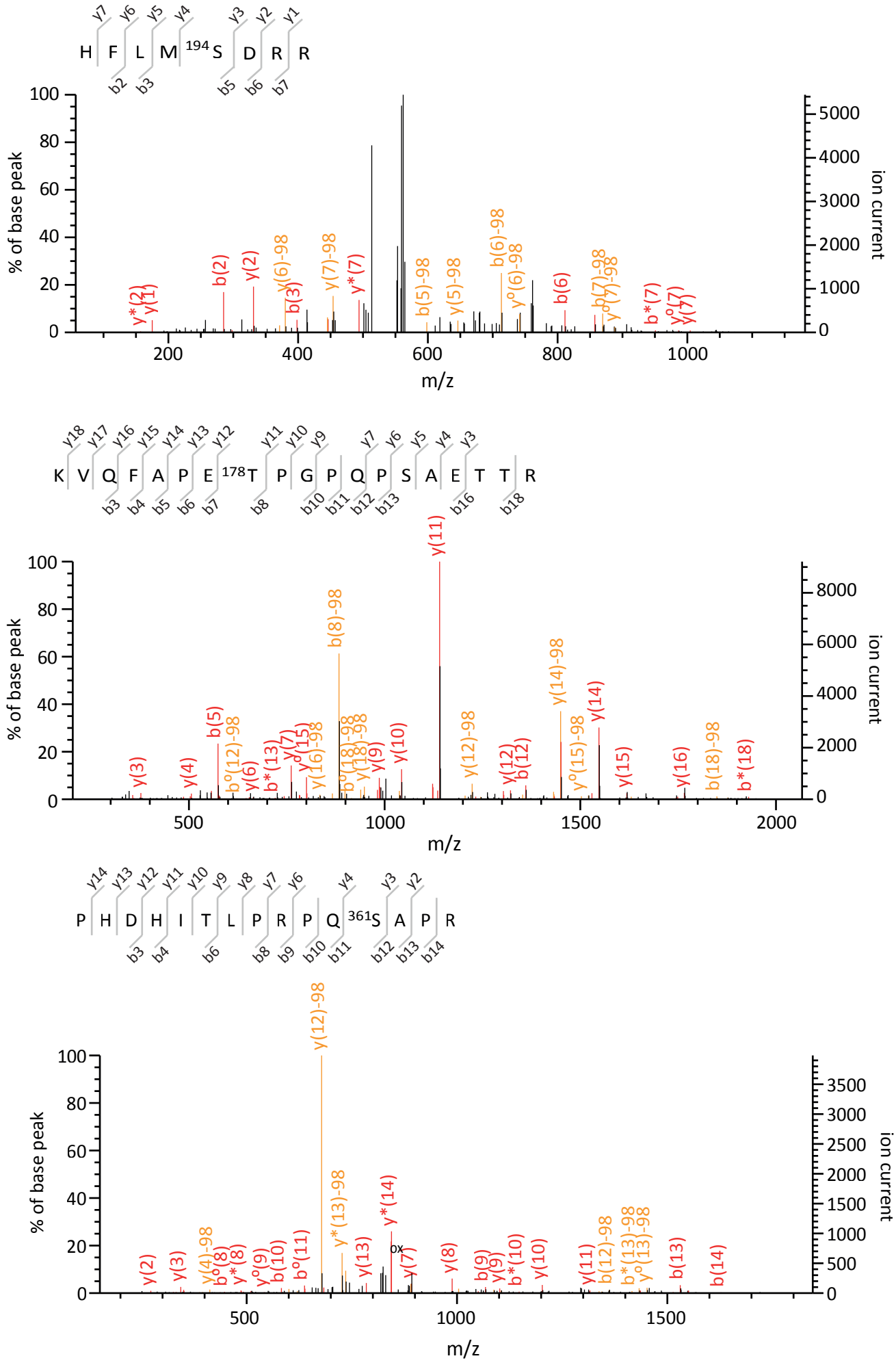

Figure 1- Figure supplement 4

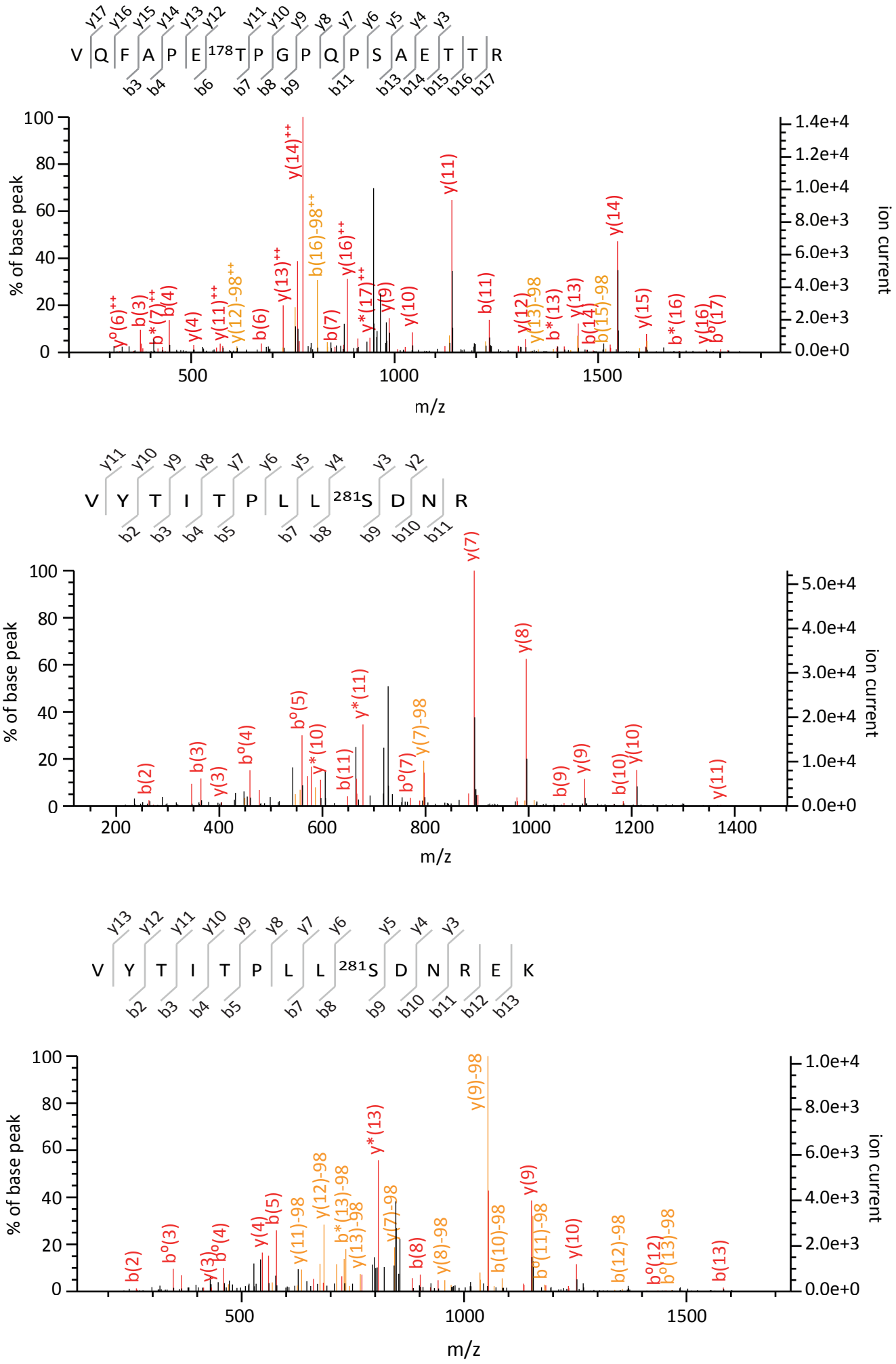

Figure 1 - Figure supplement 5

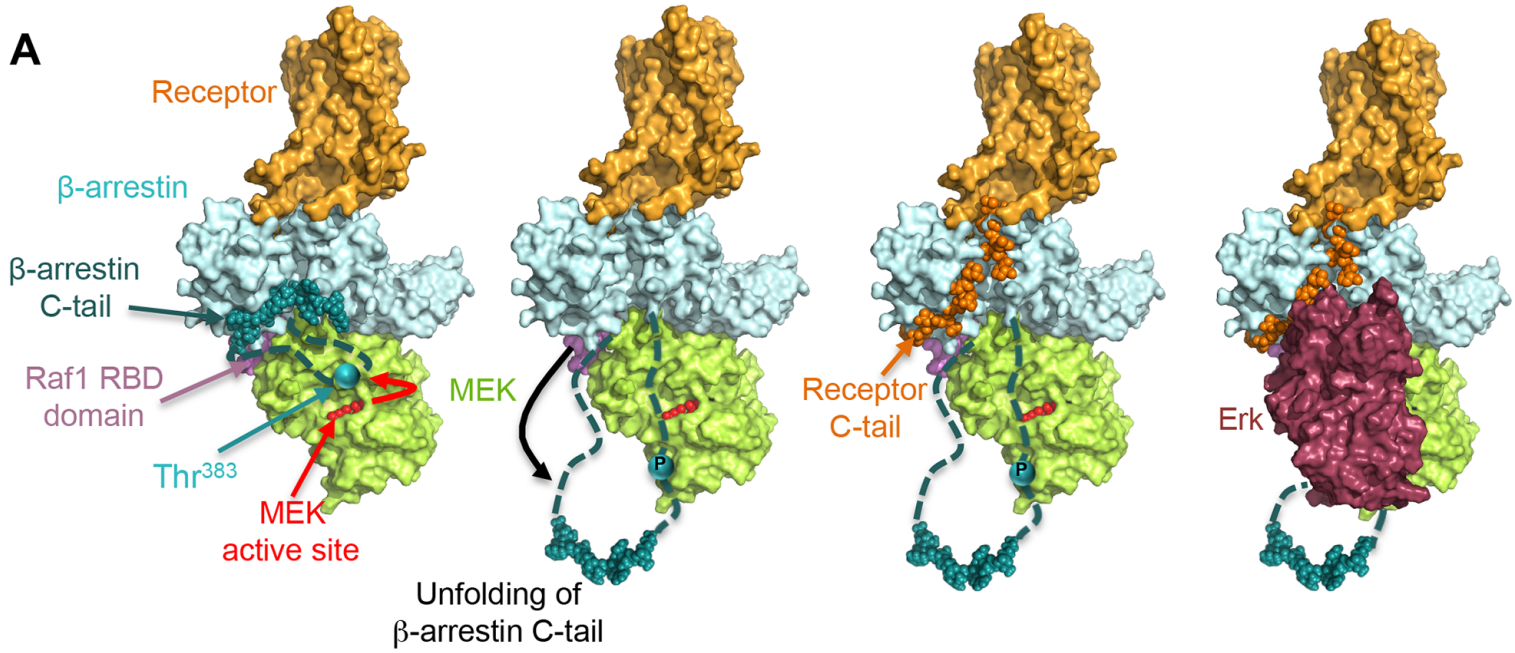
A
Receptor
β-arrestin
β-arrestin C-tail
Raf1 RBD domain
Thr383
MEK active site
MEK
Unfolding of β-arrestin C-tail
Receptor C-tail
P
Erk

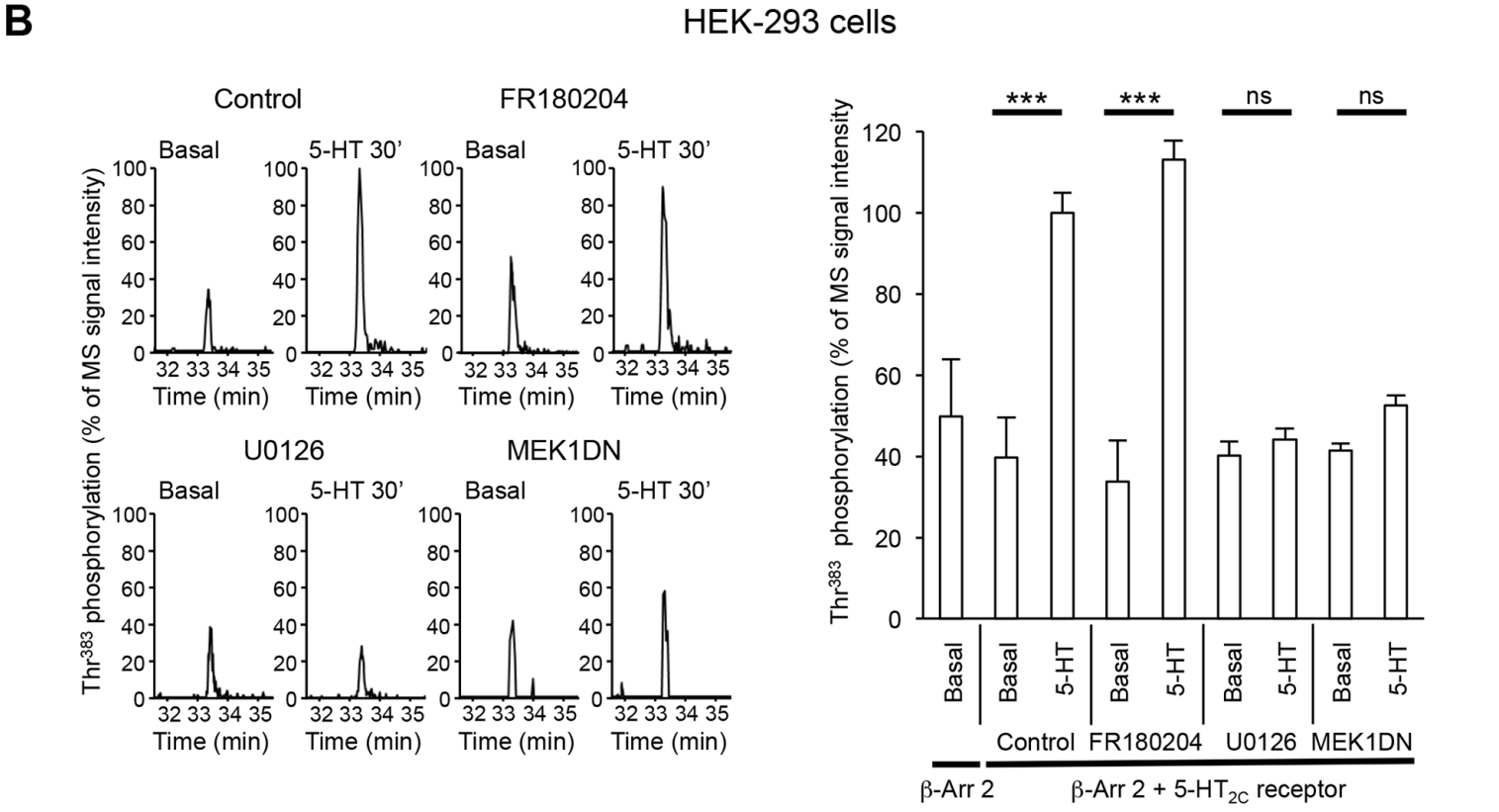
B
HEK-293 cells
Control
FR180204
U0126
MEK1DN
Basal
5-HT 30'
Thr383 phosphorylation (% of MS signal intensity)
Time (min)
***
***
ns
ns
Thr383 phosphorylation (% of MS signal intensity)
Basal
5-HT
Control
FR180204
U0126
MEK1DN
β-Arr 2
β-Arr 2 + 5-HT2C receptor

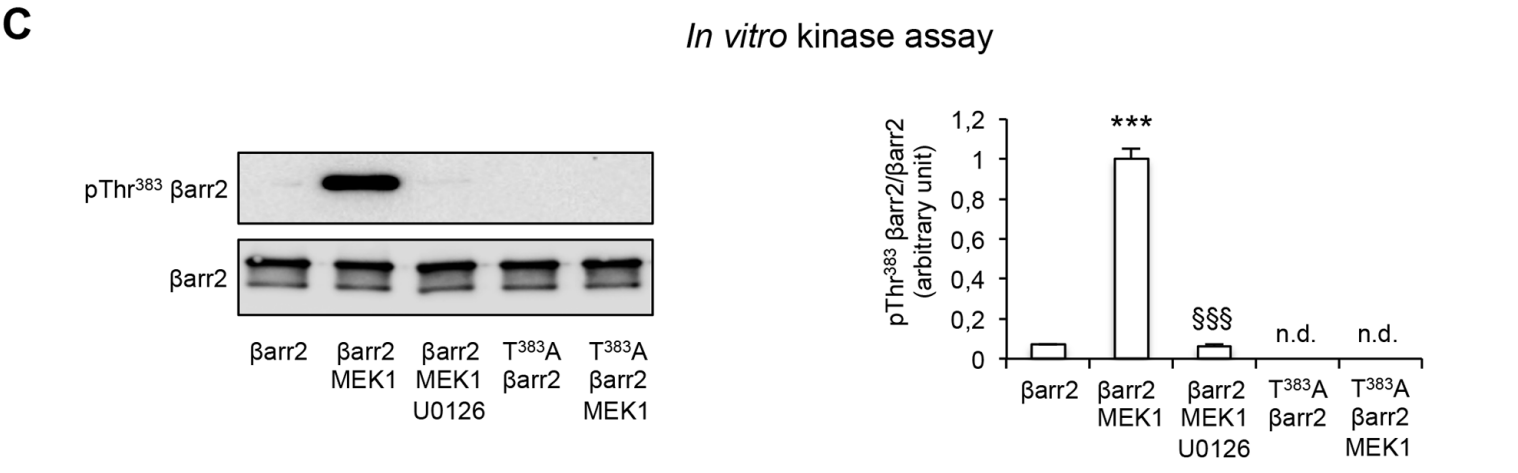
C
In vitro kinase assay
pThr383 βarr2
βarr2
βarr2
βarr2 MEK1
βarr2 MEK1 U0126
T383A βarr2
T383A βarr2 MEK1
pThr383 βarr2/βarr2 (arbitrary unit)
***
§§§
n.d.
n.d.

Figure 2

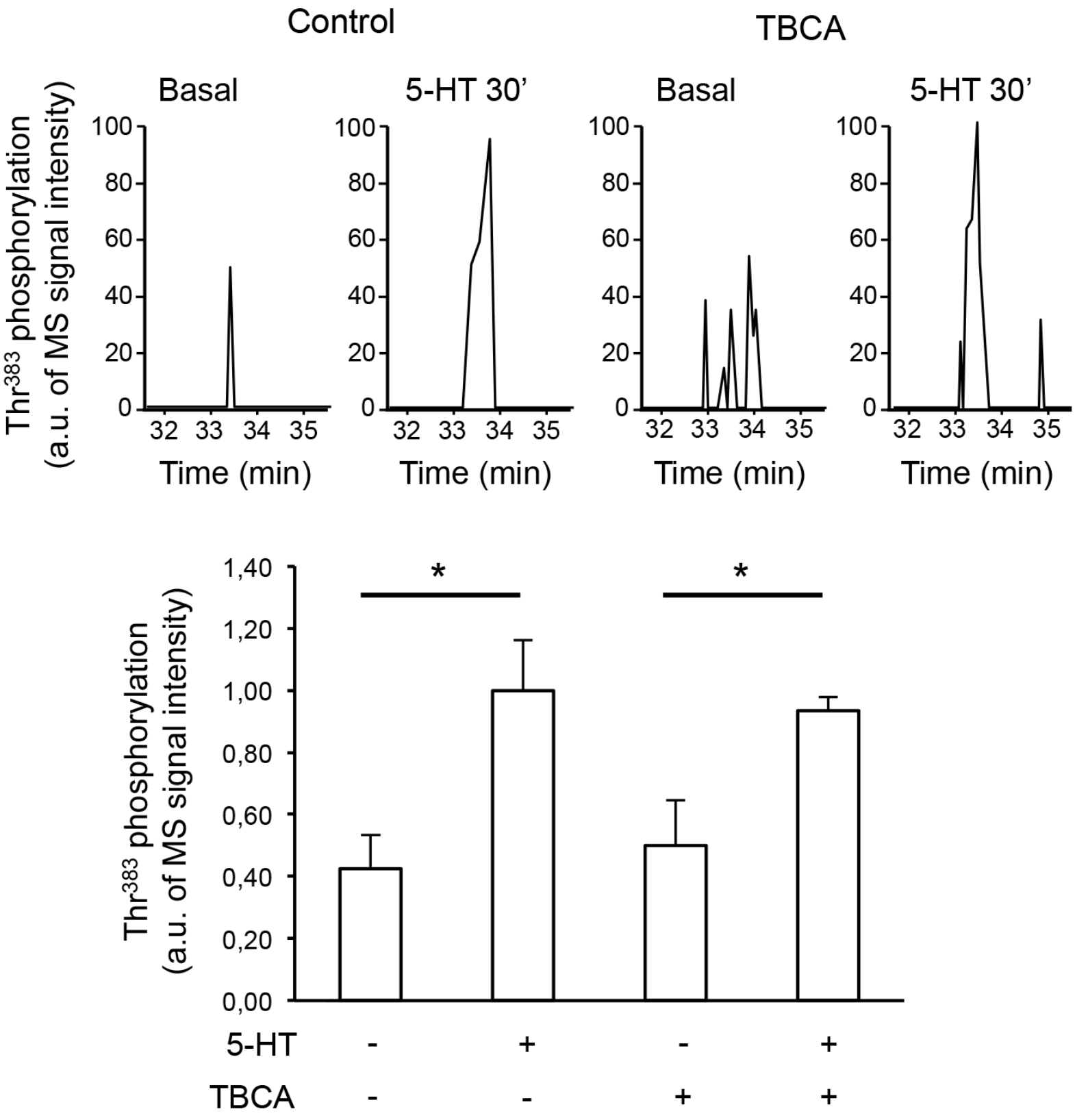

Figure 2 – Figure supplement 1

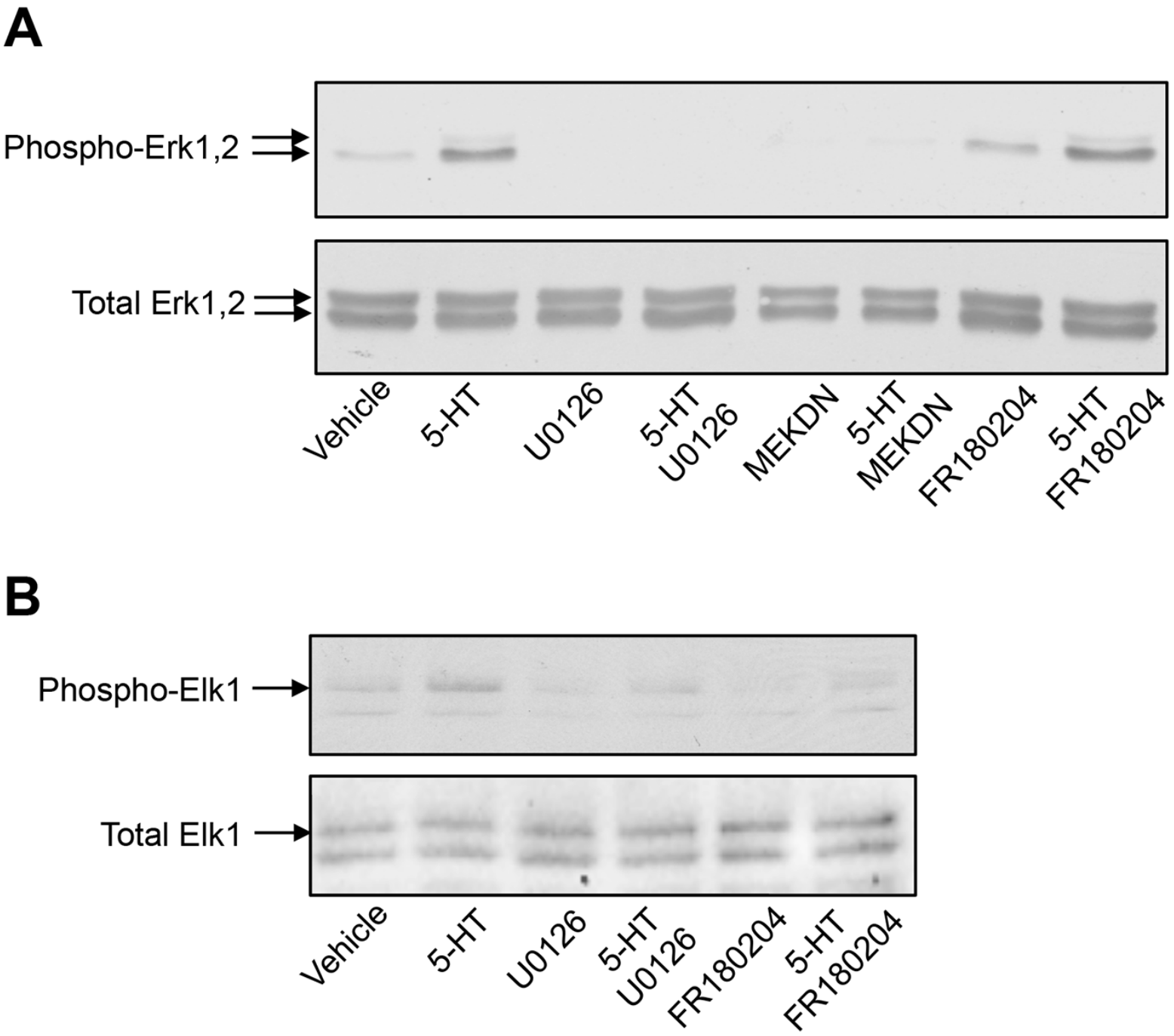

Figure 2 – Figure supplement 2

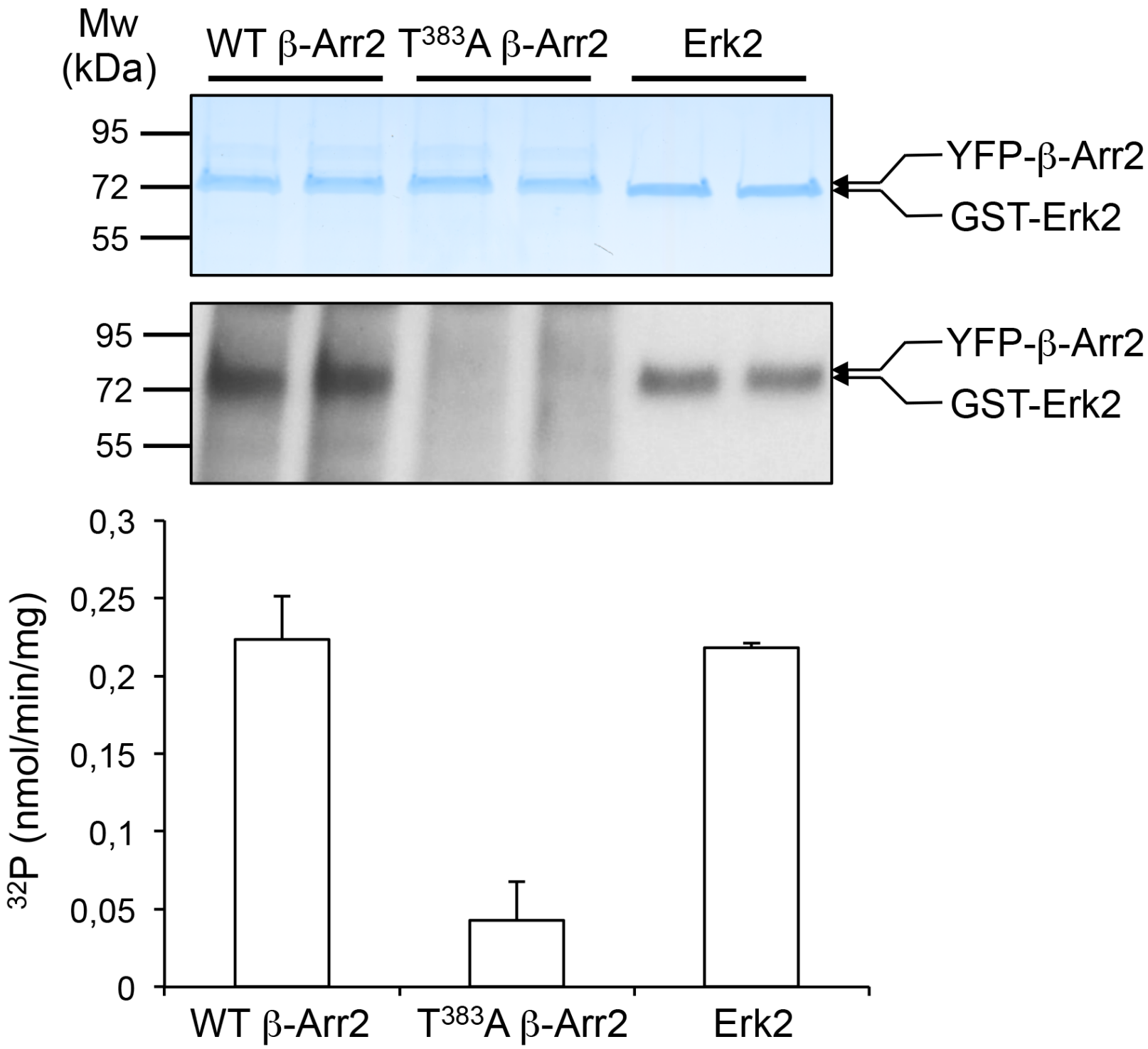

Figure 2 – Figure Supplement 3

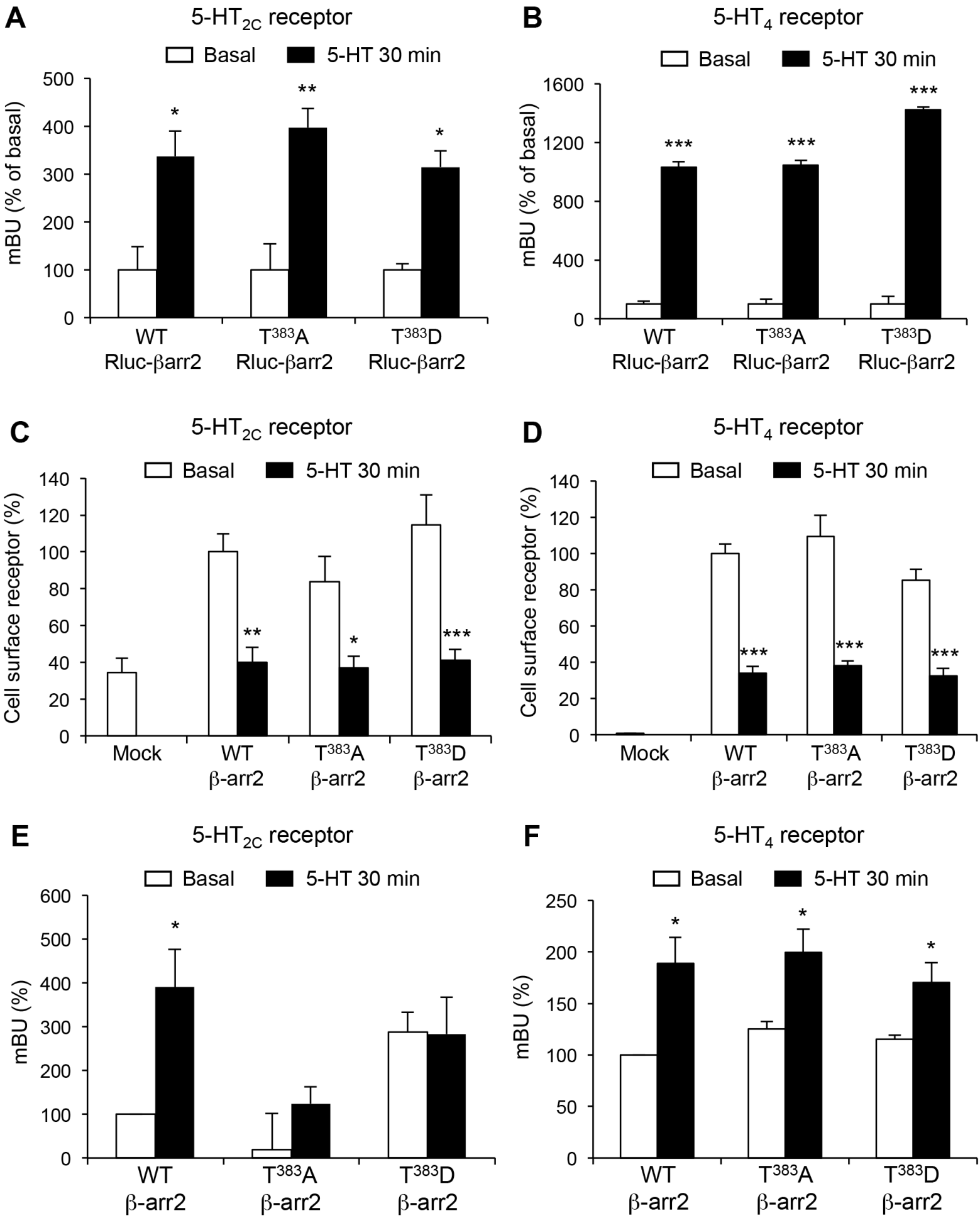
A
5-HT2C receptor
Basal
5-HT 30 min
mBU (% of basal)
500
400
300
200
100
0
*
**
*
WT Rluc-βarr2
T383A Rluc-βarr2
T383D Rluc-βarr2
B
5-HT4 receptor
Basal
5-HT 30 min
mBU (% of basal)
1600
1200
800
400
0
***
***
***
WT Rluc-βarr2
T383A Rluc-βarr2
T383D Rluc-βarr2
C
5-HT2C receptor
Basal
5-HT 30 min
Cell surface receptor (%)
140
120
100
80
60
40
20
0
**
*
***
Mock
WT β-arr2
T383A β-arr2
T383D β-arr2
D
5-HT4 receptor
Basal
5-HT 30 min
Cell surface receptor (%)
140
120
100
80
60
40
20
0
***
***
***
Mock
WT β-arr2
T383A β-arr2
T383D β-arr2
E
5-HT2C receptor
Basal
5-HT 30 min
mBU (%)
600
500
400
300
200
100
0
*
WT β-arr2
T383A β-arr2
T383D β-arr2
F
5-HT4 receptor
Basal
5-HT 30 min
mBU (%)
250
200
150
100
50
0
*
*
*
WT β-arr2
T383A β-arr2
T383D β-arr2

Figure 3

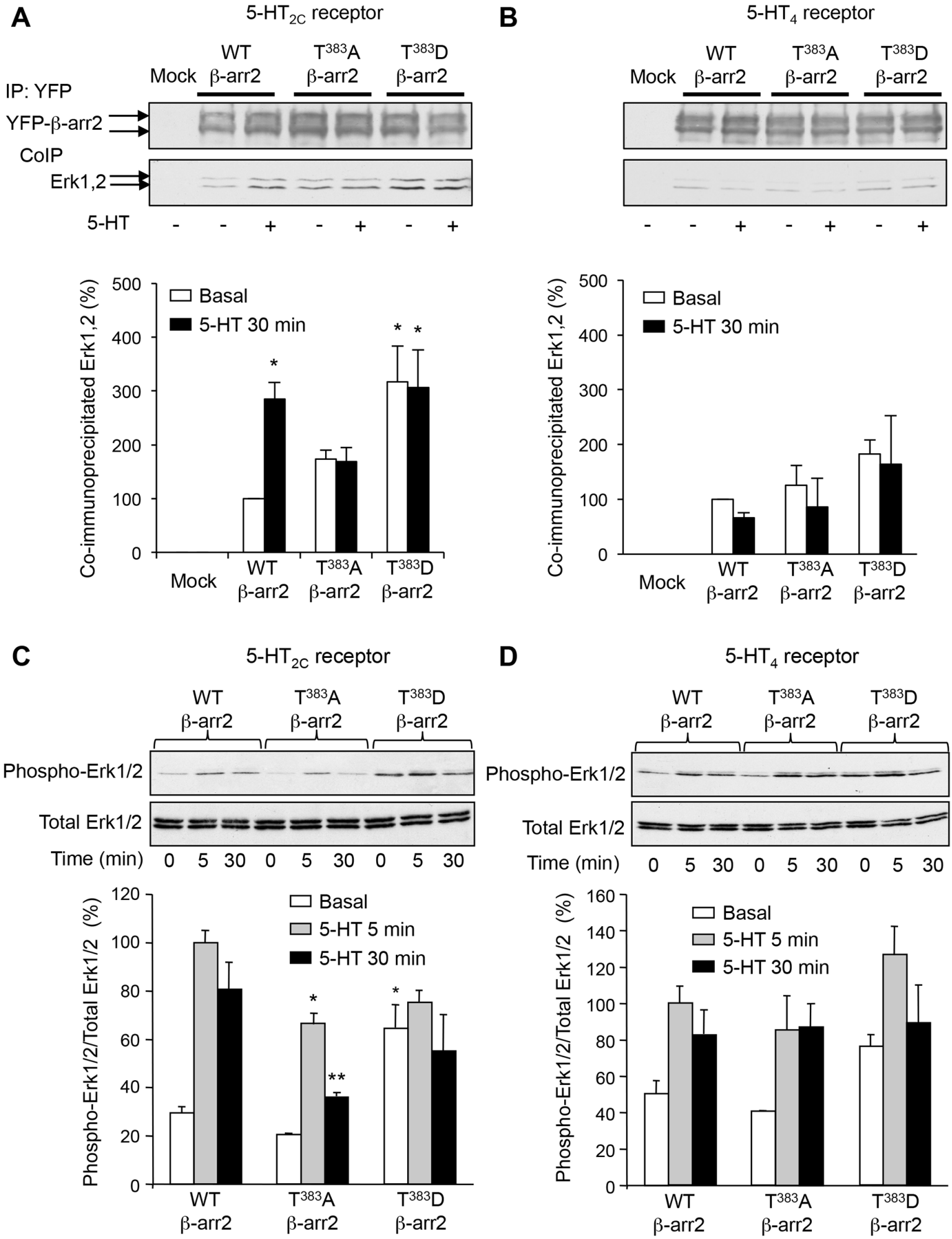
A
5-HT2C receptor
Mock
WT β-arr2
T383A β-arr2
T383D β-arr2
IP: YFP
YFP-β-arr2
CoIP
Erk1,2
5-HT
- - + - + - +
B
5-HT4 receptor
Mock
WT β-arr2
T383A β-arr2
T383D β-arr2
- - + - + - +
Co-immunoprecipitated Erk1,2 (%)
Basal
5-HT 30 min
0
100
200
300
400
500
Mock
WT β-arr2
T383A β-arr2
T383D β-arr2
C
5-HT2C receptor
Phospho-Erk1/2
Total Erk1/2
Time (min)
0 5 30 0 5 30 0 5 30
Phospho-Erk1/2/Total Erk1/2 (%)
Basal
5-HT 5 min
5-HT 30 min
0
20
40
60
80
100
120
D
5-HT4 receptor
0
20
40
60
80
100
120
140
160

Figure 4

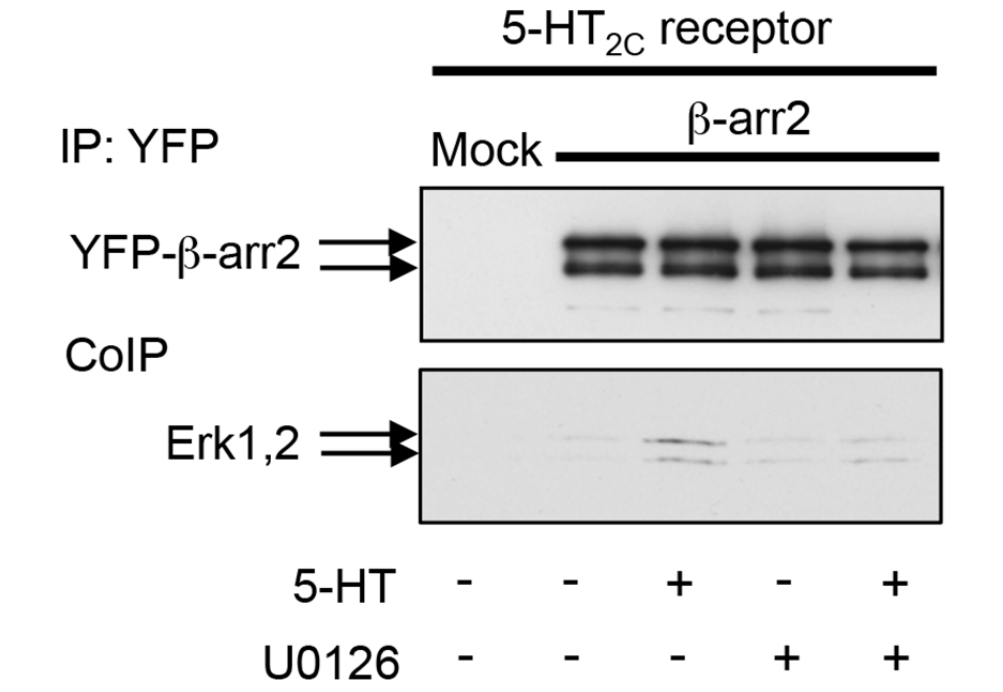

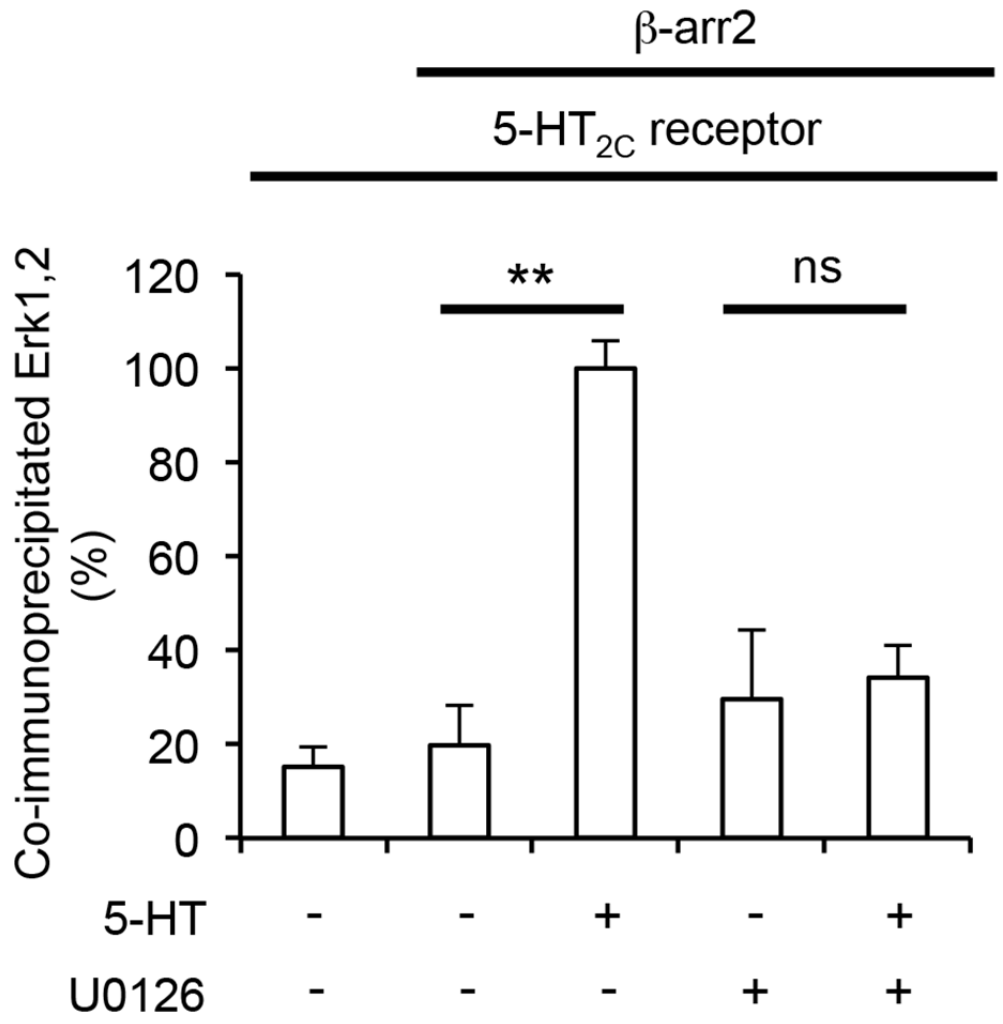

Figure 4 – Figure supplement 1

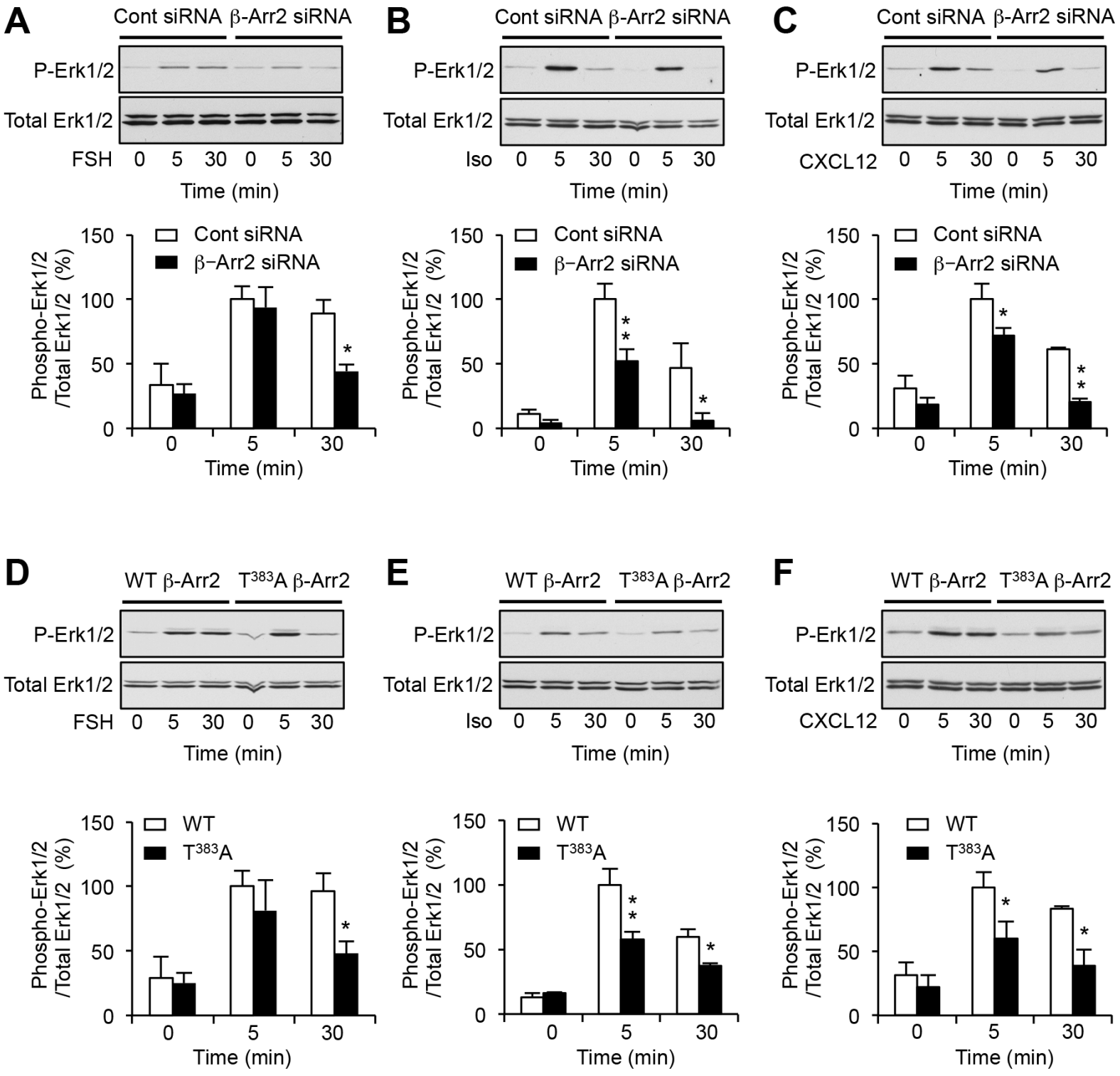
A
Cont siRNA β-Arr2 siRNA
P-Erk1/2
Total Erk1/2
FSH 0 5 30 0 5 30
Time (min)
Phospho-Erk1/2 /Total Erk1/2 (%)
Cont siRNA
β−Arr2 siRNA
B
Cont siRNA β-Arr2 siRNA
P-Erk1/2
Total Erk1/2
Iso 0 5 30 0 5 30
Time (min)
Phospho-Erk1/2 /Total Erk1/2 (%)
Cont siRNA
β−Arr2 siRNA
C
Cont siRNA β-Arr2 siRNA
P-Erk1/2
Total Erk1/2
CXCL12 0 5 30 0 5 30
Time (min)
Phospho-Erk1/2 /Total Erk1/2 (%)
Cont siRNA
β−Arr2 siRNA
D
WT β-Arr2 T383A β-Arr2
P-Erk1/2
Total Erk1/2
FSH 0 5 30 0 5 30
Time (min)
Phospho-Erk1/2 /Total Erk1/2 (%)
WT
T383A
E
WT β-Arr2 T383A β-Arr2
P-Erk1/2
Total Erk1/2
Iso 0 5 30 0 5 30
Time (min)
Phospho-Erk1/2 /Total Erk1/2 (%)
WT
T383A
F
WT β-Arr2 T383A β-Arr2
P-Erk1/2
Total Erk1/2
CXCL12 0 5 30 0 5 30
Time (min)
Phospho-Erk1/2 /Total Erk1/2 (%)
WT
T383A

Figure 5

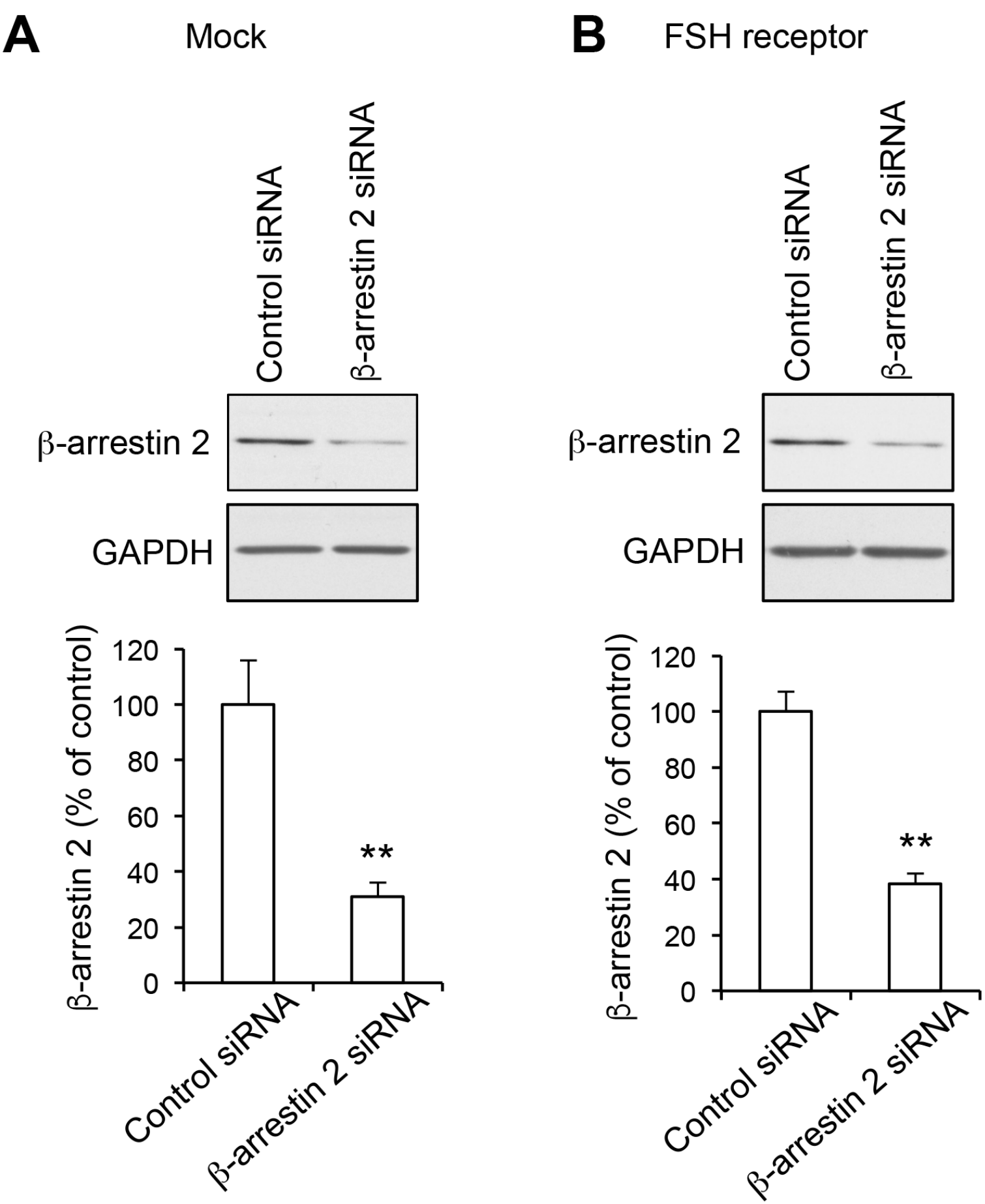

Figure 5 – Figure supplement 1

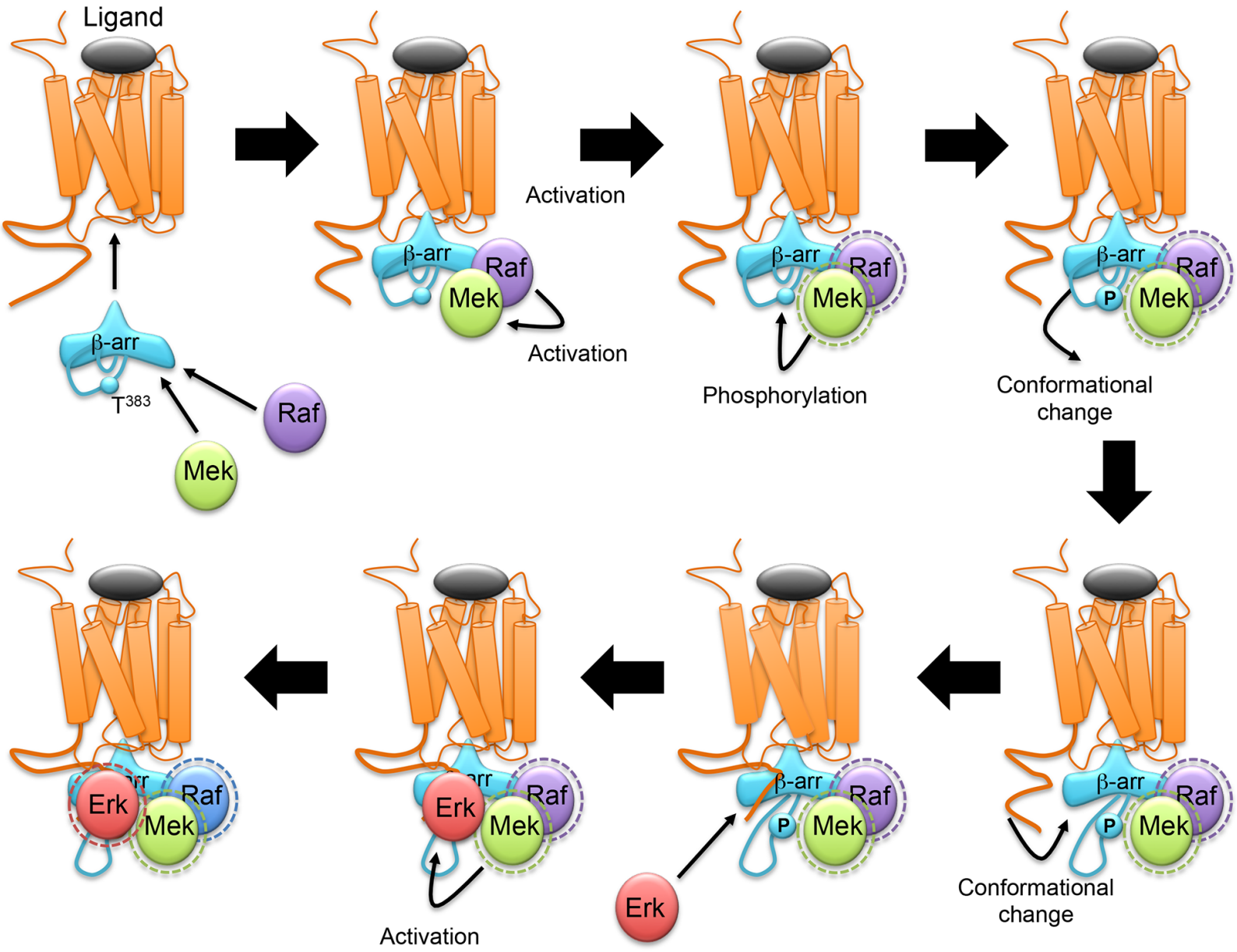
Ligand
β-arr
T383
Raf
Mek
β-arr
Raf
Mek
Activation
Activation
β-arr
Raf
Mek
Phosphorylation
β-arr
Raf
P
Mek
Conformational change
β-arr
Raf
P
Mek
Conformational change
Erk
β-arr
Raf
P
Mek
Erk
Raf
Mek
Activation
Erk
Raf
Mek

Figure 6